



Cite this: *Chem. Soc. Rev.*, 2021, 50, 12808

Recent advances in transition-metal-catalysed asymmetric coupling reactions with light intervention

Fu-Dong Lu,^{†a} Jun Chen,^{†a} Xuan Jiang,^{†a} Jia-Rong Chen,^{ID a} Liang-Qiu Lu^{ID *a} and Wen-Jing Xiao^{ID *ab}

Transition metal-catalysed asymmetric coupling has been established as a robust tool for constructing complex organic molecules. Although this area has been extensively studied, the development of efficient protocols to construct stereogenic centres with excellent regio- and enantioselectivities is highly desirable and remains challenging. Asymmetric transition metal catalysis with light intervention provides a practical alternative strategy to current methods and considerably expands the synthetic utility as a result of abundant feedstocks and mild conditions. This tutorial review comprehensively summarizes the recent advances in transition-metal-catalysed asymmetric coupling reactions with light intervention; in particular, a concise analysis of substrate scope and the mechanistic scenarios governing stereocontrol is discussed.

Received 26th February 2021

DOI: 10.1039/d1cs00210d

rsc.li/chem-soc-rev

1. Introduction

Asymmetric catalysis is the most economical and efficient method to achieve chiral functional molecules such as chiral medicines, pesticides and materials. In recent years, the application of emerging methods and strategies has greatly promoted the development of asymmetric catalysis. For example, radical

reactions driven by visible light have become an important part of the field of catalytic organic synthesis due to their high efficiency and mildness, and green properties.^{1–6} The application of visible-light photocatalysis to asymmetric catalysis is bound to create a promising field in organic synthesis and provide new opportunities for asymmetric synthesis. In 2008, MacMillan successfully combined visible-light photocatalysis with asymmetric amine catalysis, thereby addressing the difficult stereocontrol of free radical reactions and laying the foundation for the later development of photoinduced asymmetric organic synthesis.⁷ Since then, the reaction types and chemical feedstocks have been greatly enriched by combining photocatalysis with a variety of asymmetric catalysis strategies, including carbene catalysis,⁸ Brønsted acid catalysis,^{9,10} transition-metal

^a CCNU-uOttawa Joint Research Centre, Key Laboratory of Pesticide and Chemical Biology, Ministry of Education, College of Chemistry, Central China Normal University, 152 Luoyu Road, Wuhan 430079, China.

E-mail: luliangqiu@mail.ccnu.edu.cn, wjxiao@mail.ccnu.edu.cn

^b State Key Laboratory of Organometallic Chemistry, Shanghai Institute of Organic Chemistry, 345 Lingling Road, Shanghai 200032, China

[†] These authors contribute equally to this work.



Fu-Dong Lu

Fu-Dong Lu was born in Shandong Province, China, in 1995. He received his BS in Chemistry from Huazhong Agricultural University in 2017. Currently, he is carrying out his doctoral studies on visible-light-catalysed asymmetric coupling reactions under the direction of Prof. Liang-Qiu Lu and Prof. Wen-Jing Xiao at the Central China Normal University.



Jun Chen

Jun Chen was born in Hubei Province, China, in 1992. He received his BS from Hubei Normal University. In 2015, he began his PhD studies under the supervision of Prof. Jia-Rong Chen and Prof. Wen-Jing Xiao at CCNU. His research interests are asymmetric catalysis and photocatalysis.

catalysis,^{11,12} and Lewis acid catalysis,¹³ as well as bifunctional photoredox/asymmetric catalysis with a single catalyst (Fig. 1).^{14,15}

Among the many currently developed strategies for asymmetric photochemical synthesis, dual and bifunctional photoredox and transition metal catalysis is the most mature and diverse. This achievement is undoubtedly attributed to the increasing number of chemists working on transition metal catalysis in recent decades. Compared with traditional transition-metal catalysed coupling reactions, the introduction of the photoredox catalysis strategy makes the reaction milder and greener and enables the reactivity of free radicals, which are open-shell active species, to be precisely controlled, providing a new way to synthesize chiral molecules. This review comprehensively summarizes the advances in transition metal-catalysed asymmetric coupling reactions with light intervention according to the classification of transition metals (Scheme 1).

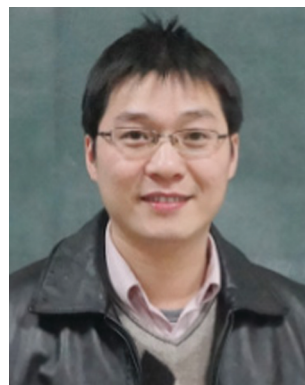
2. Photoinduced asymmetric coupling reactions with a chiral nickel catalyst

Transition metal catalysis has brought a profound impact on science and society. In the 21st century, the Nobel Prize in Chemistry has been awarded to scientists who have made outstanding contributions to transition metal catalysis.^{16–18} Among them, nickel-catalysed coupling reactions (such as the Suzuki–Miyaura reaction) have been well developed due to their powerful ability to build C–C bonds.^{19,20} However, although this type of reaction can achieve efficient construction of C_{sp²}–C_{sp²} bonds, there are still great challenges in the construction of C_{sp³} chiral centres due to the slow rates of oxidative addition and transmetalation and the proneness to β-hydride elimination of alkyl metallic species.^{21–23} In this regard, the nickel-catalysed asymmetric coupling reaction between alkyl halides and organometallic nucleophiles mainly from Fu's group, which proceeds



Xuan Jiang

Xuan Jiang was born in Zhejiang Province, China, in 1994. He received his master's degree in Central China Normal University in 2019 and is now pursuing his doctoral degree under the supervision of Prof. Liang-Qiu Lu and Prof. Wen-Jing Xiao. His research interests are focused on visible light photoredox catalysis and radical carbonylation.



Jia-Rong Chen

Jia-Rong Chen earned his PhD from the CCNU under the supervision of Prof. Wen-Jing Xiao in 2009. After holding a position at CCNU in 2009–2010, he worked as a Humboldt Postdoctoral Fellow with Prof. Carsten Bolm at the RWTH Aachen University in 2011–2012. In 2012 he returned to CCNU to begin his independent career as an associate professor and was promoted to full professor in 2016. His research interests include photoredox catalysis, nitrogen radical chemistry, and asymmetric catalysis.



Liang-Qiu Lu

Liang-Qiu Lu was born in Zhejiang Province, China, in 1982. He obtained his PhD degree from Central China Normal University (CCNU) under the supervision of Professor Wen-Jing Xiao (2011). Subsequently he worked as a Humboldt postdoctoral fellow with Prof. Matthias Beller in Leibniz Institute for Catalysis (2011–2013). In June 2015, he was exceptionally promoted to professor. His research interests focus on green synthesis and asymmetric catalysis.



Wen-Jing Xiao

Wen-Jing Xiao was born in Hubei Province, China, in 1965. He received his MSc in chemistry from Central China Normal University (CCNU) under the supervision of Professor Wen-Fang Huang (1990). In 2000, he received his PhD degree under the direction of Professor Howard Alper in University of Ottawa, Canada. Subsequently he worked as a postdoctoral researcher in the lab of Prof. David W. C. MacMillan (2001–2002) in California Institute of Technology (US). In 2003, Dr Xiao became a full professor in the College of Chemistry at CCNU, China. His current research interests focus on the discovery of new methodology for carbo- and heterocyclic molecules.

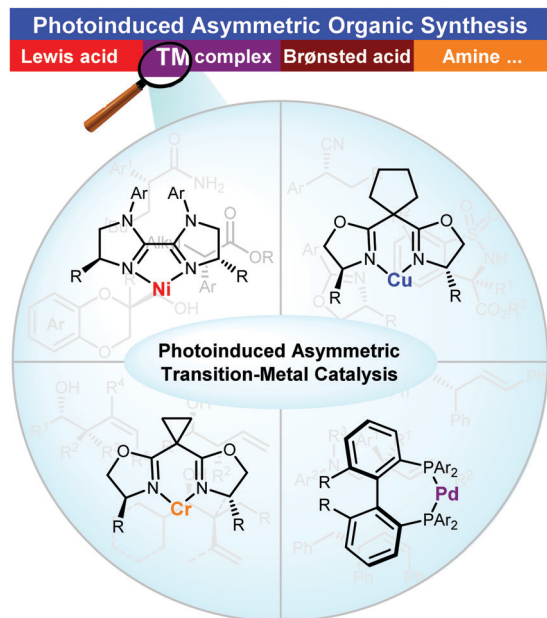
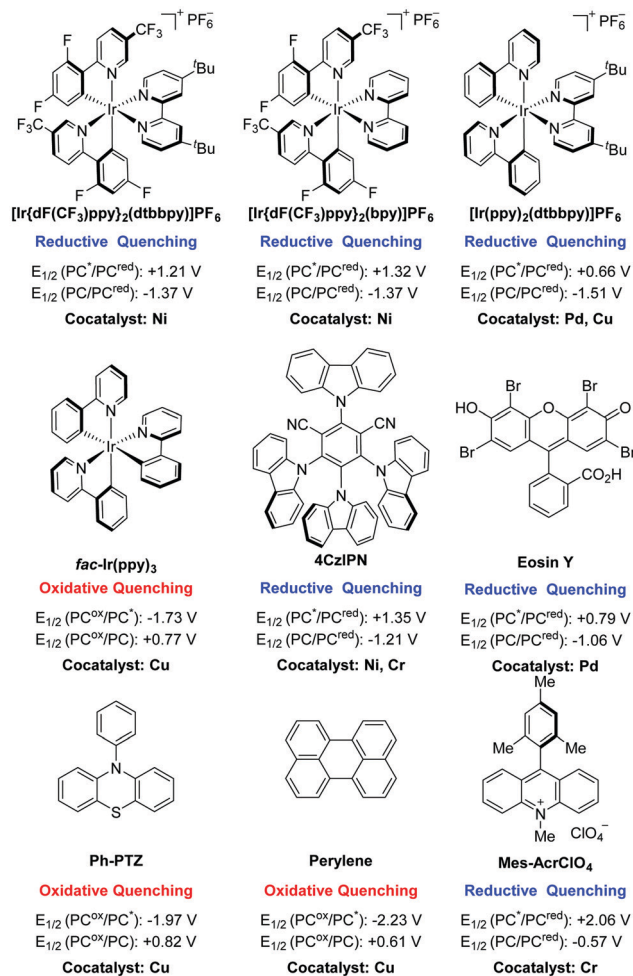


Fig. 1 Transition-metal-catalysed asymmetric couplings with light intervention.

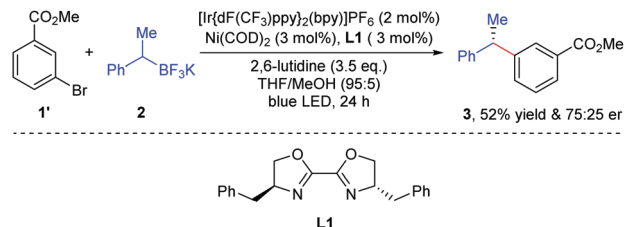
through transient radical species, provides new ideas for addressing this challenge in the past decade.^{24–26} Despite great achievements, this strategy also suffers somewhat from shortcomings, such as the use of moisture- and oxygen-sensitive organometallic reagents and limited alkyl halides as radical precursors. In addition, the generation of carbon radicals through photocatalytic single electron transfer (SET) and the subsequent capture of the radicals by metal species provide a new gentle and efficient way for the nickel catalyzed construction of C_{sp^3} -stereogenic centres. This metallaphotoredox catalysis strategy not only avoids the use of organometallic reagents, but also allows more bench-stable and inexpensive radical precursors to participate in the reaction, such as carboxylic acids, simple C_{sp^3} -H bonds, and so on. At the same time, since the radical addition step increases the metal valence, the metal species must undergo subsequent single electron reduction to maintain the redox neutrality of the reaction. The combination of photoredox catalysis and nickel catalysis can achieve free radical generation while reducing the metal valence under mild conditions.

In 2014, Molander *et al.*²⁷ and Doyle and MacMillan *et al.*²⁸ independently reported the first C_{sp^3} - C_{sp^2} cross-coupling reaction through synergistic photocatalysis and nickel catalysis. Notably, Molander realized the first asymmetric cross-coupling reaction using this strategy. In the presence of the photocatalyst $Ir[dF(CF_3)ppy]_2(bpy)PF_6$ and the chiral $Ni/L1$ catalyst, aryl halide **1'** and racemic potassium benzyl trifluoroborate **2** were converted to chiral 1,1-diarylethane products **3** in 52% yield and a 75:25 enantiomeric ratio (Scheme 2).

This experiment not only verifies that photocatalytic transition metal catalysis can be used to construct chiral compounds, but also provides evidence that the radical is captured by the ligated Ni complex. Therefore, the following single-electron transmetalation mechanism was proposed for this photoredox cross-coupling

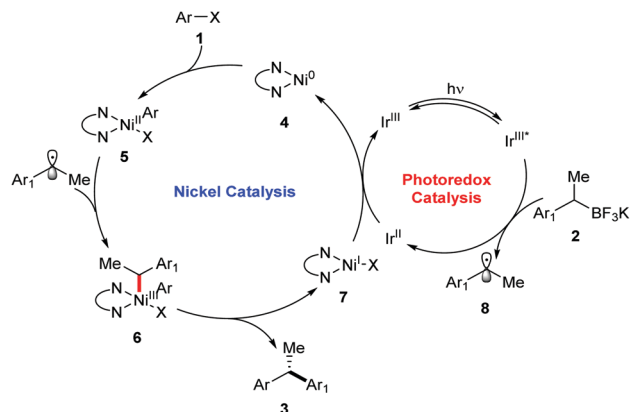


Scheme 1 Common photocatalysts and their transition metal cocatalysts.



Scheme 2 Photoredox/nickel-catalysed asymmetric cross-coupling of benzylic trifluoroborates with aryl bromides.

reaction (Scheme 3). First, the ground-state $Ir(III)$ catalyst reaches the excited state under irradiation. Potassium benzyl trifluoroborate gives a single electron to the excited-state $Ir(III)^*$ to form alkyl radical **8** while generating reduced photocatalyst $Ir(II)$. The alkyl radical is then captured by the $Ni(II)$ complex, which is produced by the oxidative addition between the aryl halide and $Ni(0)$ catalyst to yield high-valent nickel intermediate **6**. Reductive elimination of intermediate **6** delivers the final product, and the $Ni(I)$ species, which is subsequently reduced to $Ni(0)$ by reduced photocatalyst $Ir(II)$, encloses both the photocatalytic and Ni -catalysed cycles. The completion of this work

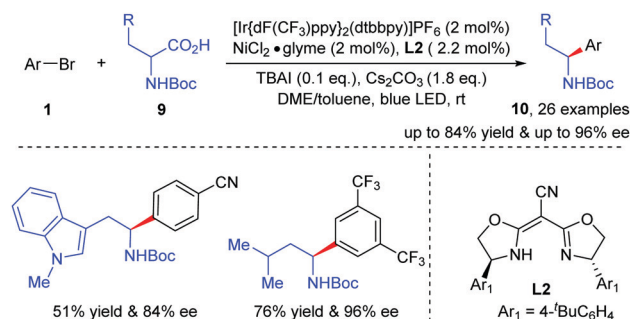
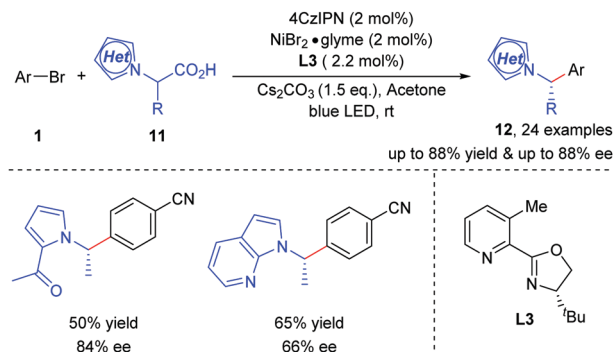
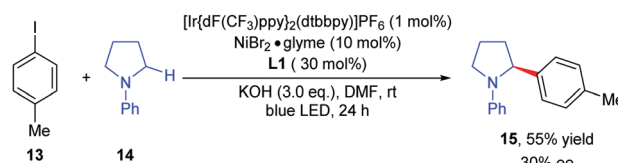


Scheme 3 Mechanism of the photoredox/nickel-catalysed cross-coupling.

undoubtedly laid a solid foundation for the later metallaphotoredox-catalysed asymmetric cross-coupling reactions. In 2016, Molander discovered that acyl chlorides can also participate in photoredox/nickel-catalysed asymmetric coupling reactions, thereby realizing the construction of a chiral centre at the α -position of the carbonyl group.²⁹

In 2016, MacMillan and Fu reported an asymmetric decarboxylative arylation of α -amino acids by combining enantioselective nickel catalysis with photoredox catalysis (Scheme 4).³⁰ A series of readily available α -amino acids **9** were converted to chiral benzylic amine compounds **10** in high yields and high enantioselectivities. It is worth noting that this dual catalysis system not only has a wide substrate scope but also enables the construction of the core skeletons of some pharmacologically active molecules, which shows the utility of this asymmetric cross-coupling reaction.

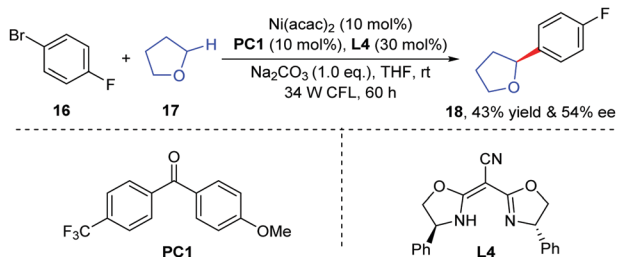
In addition to α -amino acids, in 2019 Davidson disclosed a photoredox/nickel-catalysed asymmetric decarboxylative arylation of α -heterocyclic carboxylic acids (Scheme 5). With PyOx as the ligand, a variety of chiral *N*-benzylic heterocycles (with up to 88% ee) were synthesized.³¹ In contrast, when α -heterocyclic carboxylic acids **11** contain carbonyl, pyridine or other directing groups, the enantioselectivity is better than that in the case of those that lack directing groups in many cases. The directing group can result in the chelation of alkyl radicals and nickel species occurring in closer proximity, thereby enabling easier control over the enantioselectivity.

Scheme 4 Photoredox/nickel-catalysed enantioselective decarboxylative arylation of α -amino acids.Scheme 5 Photoredox/nickel-catalysed enantioselective synthesis of *N*-benzylic heterocycles.

Scheme 6 Photoredox/nickel-catalysed enantioselective C–H arylation.

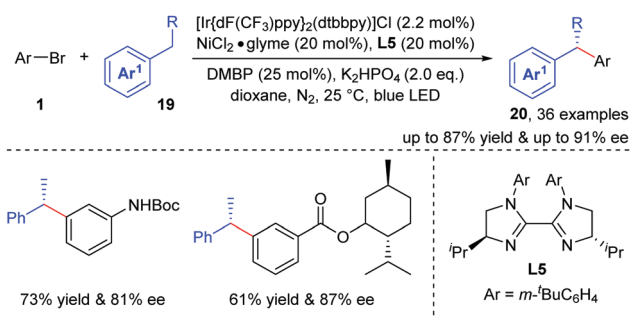
The functionalization of C–H bonds that are widespread in organic molecules is undoubtedly the most direct, economical and efficient route to add the molecular complexity. In 2016, Doyle *et al.* reported a direct α -C(sp³)–H functionalization of amines with aryl halides through synergistic photoredox/nickel catalysis, which led to an efficient synthesis of benzylic amines.³² In this work, α -amino radicals are generated *via* the single-electron oxidation of amines by the excited-state photocatalyst, followed by deprotonation. Chiral product **15** is formed with modest enantioselectivity when a chiral BiOx ligand is used in the reaction (Scheme 6).

In addition to the abovementioned oxidative deprotonation, direct hydrogen atom transfer (HAT) is another efficient way to generate carbon radicals. In 2018, Martin *et al.* achieved direct C(sp³)–H arylation and alkylation at the α -position to the oxygen by combining triplet ketone catalysis with nickel catalysis.³³ When diaryl ketones are used as photosensitizers, this enables not only hydrogen atom extraction but also SET to recycle nickel catalysts. The catalytic cycle starts from the HAT process initiated by the triplet ketone catalyst, which produces both carbon radicals from ethers and ketyl radicals from ketone catalysts. Concurrently, oxidative addition between the aryl halides and low-valent Ni(0) catalyst occurs to generate Ni(II) species. The nucleophilic carbon radicals are then captured by Ni(II) species to generate Ni(III), which undergoes reductive elimination to deliver the targeted C–H arylation product. Notably, the presence of electron-donating and electron-accepting groups on the diaryl ketone catalyst significantly improves the reaction efficiency. The reason is that these groups can result in the redshift of the absorption wavelength of the catalyst, adjust the decay rate of the triplet excited state and stabilize the ketyl radicals. When the chiral nickel catalyst was applied, chiral α -aryl-substituted tetrahydrofuran could be obtained in moderate yield and enantioselectivity (Scheme 7).



Scheme 7 Photoredox/nickel-catalysed enantioselective C–H arylation of furan.

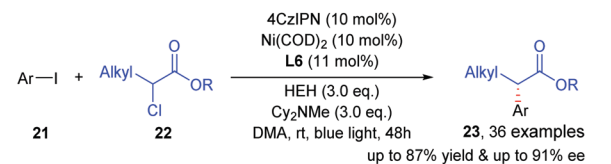
Different from the aforementioned HAT- and nickel-catalysed asymmetric coupling reactions, Lu *et al.* achieved a photoredox/nickel-catalysed enantioselective benzylic C–H arylation (Scheme 8).³⁴ A series of chiral 1,1-diaryl alkanes that are key skeletons in natural products were obtained in high yields and with good enantioselectivities. The newly developed chiral biimidazoline (BiIM) ligands play an important role in improving the enantioselectivity of the reaction. Compared with bioxazoline (BiOX) ligands, BiIM ligands adjust the electrical properties and steric hindrance more facilely, making it easier to regulate the enantioselectivity. Like most photoredox/nickel-catalysed couplings, this reaction undergoes an oxidative addition to generate Ni(II) species. However, these aryl Ni(II) species generated through the oxidative addition of aryl bromides to Ni(0) species do not directly capture the free radical species, but are oxidized by the excited-state photocatalysts to generate bromine radicals, new aryl Ni(II) species and the reduced Ir(II) photocatalysts. In the presence of a base and bis(4-methoxyphenyl)methanone (DMBP),



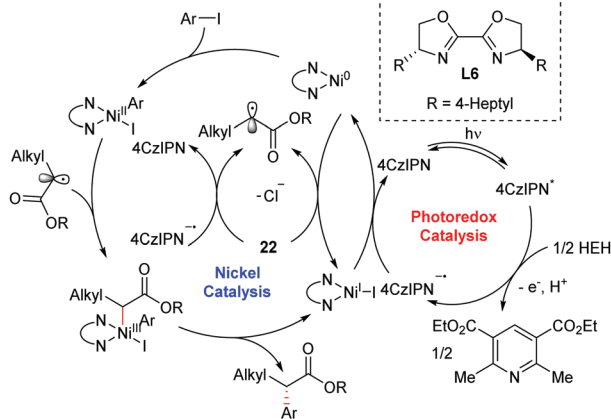
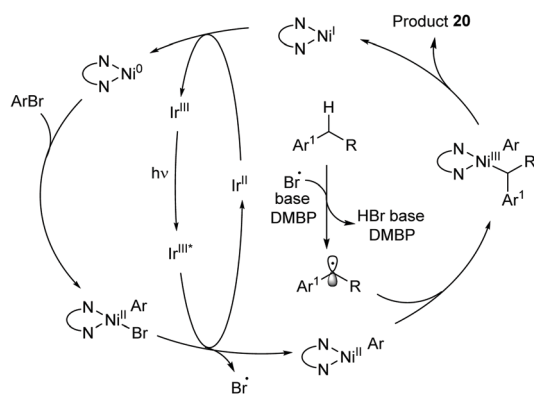
Scheme 8 Photoredox/nickel-catalysed enantioselective benzylic C–H arylation.

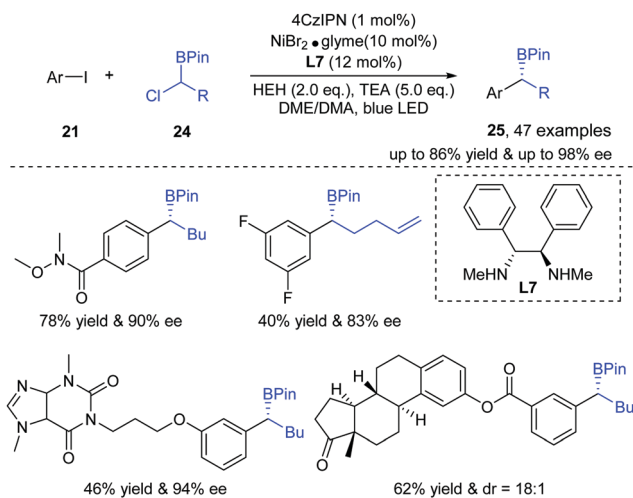
bromine radicals abstract the benzylic hydrogen from alkyl benzene to form benzylic radicals which are then trapped by aryl Ni(II) species to form Ni(III) species. The Ni(III) species then undergo reductive elimination to form the final chiral 1,1-diaryl alkanes and Ni(I) species. The SET between the reduced photocatalysts and Ni(I) species would link the photocatalysis and Ni catalysis cycles. Significantly, this strategy provides not only an efficient method with high atom economy for the synthesis of chiral 1,1-diaryl alkanes, but also a means for the synthesis and modification of natural products and drugs with similar structures.

In 2019, Mao reported a photoredox/nickel-catalysed asymmetric reductive cross-coupling between α -chloro ester **22** and aryl iodides **21** with Hantzsch esters (HEH) as the reducing agents, leading to valuable chiral α -aryl esters **23** in high yields and enantioselectivities (Scheme 9).³⁵ Initially, Ni(0) and aryl iodides undergo oxidative addition to form aryl Ni(II) species which then capture the α -carbonyl radicals in a stereoselective manner to form Ni(III) species. Carbonyl radicals are produced by the reduction of α -chloro esters by the reduced photocatalyst 4CzIPN^{•-} or Ni(0). After that, reductive elimination of Ni(III) species delivers the final chiral α -aryl esters and Ni(I) species, the latter of which are then reduced by the reduced photocatalyst to regenerate the Ni(0) species and close the two catalytic cycles. This reaction not only has a wide substrate scope for both coupling agents but also avoids the use of stoichiometric metal reducing agents. Recently, Xu *et al.* also realized an asymmetric reductive coupling reaction between aryl iodides and α -chloroboranes through a similar strategy (Scheme 10).³⁶ This strategy realizes the efficient and high enantioselective synthesis of benzyl borate under mild conditions, and has good functional group compatibility, which provides a new idea for the synthesis of chiral boron compounds.

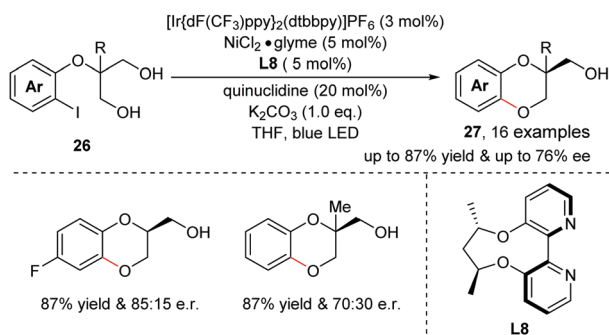


Scheme 9 Photoredox/nickel-catalysed asymmetric reductive cross-coupling.





Scheme 10 Photoredox/nickel-catalysed asymmetric reductive cross-coupling between aryl iodides and α -chloroboranes.

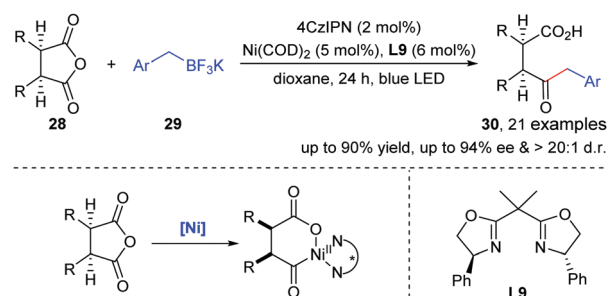


Scheme 11 Photoredox/nickel-catalysed desymmetric C–O coupling.

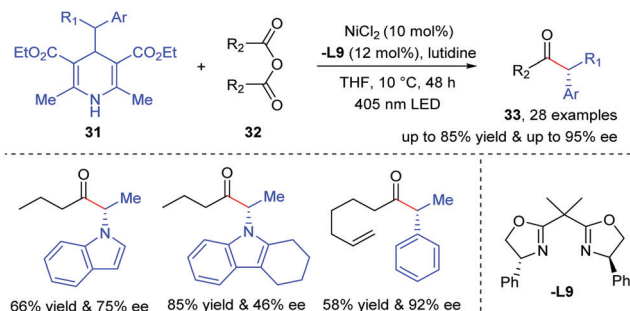
The Ni(II) species can not only capture radicals to form Ni(III) species but also can be directly oxidized by photocatalysts to increase the valence of the metal to promote reductive elimination. In 2018, Xiao *et al.* reported a desymmetric C–O coupling reaction through dual photoredox and nickel catalysis, converting prochiral 1,3-diol to chiral 1,4-benzodioxanes **27** which are the core skeletons of many natural products (Scheme 11).³⁷ Axially chiral 2,2'-bipyridine ligands play an important role in maintaining the high yield and controlling the enantioselectivity of the reaction.

In addition to aryl halides, anhydrides and acyl chlorides can be used as efficient electrophiles in metallaphotoredox-catalysed coupling reactions. In 2017, Doyle and Rovis *et al.* disclosed a photoredox/nickel-catalysed desymmetrization of meso-anhydrides **28**, obtaining chiral β -keto acids **30** in good enantio- and diastereoselectivities (Scheme 12).³⁸ This reaction is mainly achieved by the oxidative addition of Ni(0) by anhydride to generate acyl Ni(II) species. They can capture radicals and undergo reductive elimination to deliver the desired products.

Recently, HEH substrates have been widely used as radical precursors in photocatalytic coupling reactions.³⁹ Such radical precursors can not only be oxidized by a photocatalyst to generate alkyl radicals but also be directly excited by light to generate free radicals. In a recent publication, Melchiorre and



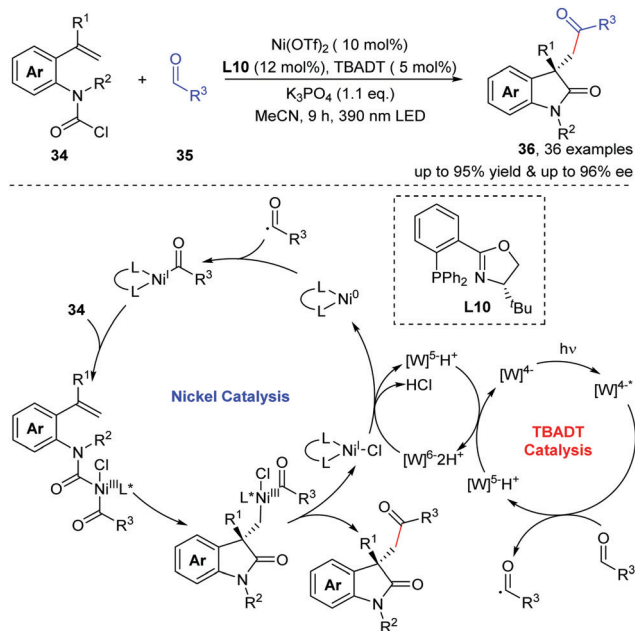
Scheme 12 Photoredox/nickel-catalysed enantioselective desymmetrization of cyclic meso-anhydrides.



Scheme 13 Photoredox/nickel-catalysed asymmetric acyl cross-coupling.

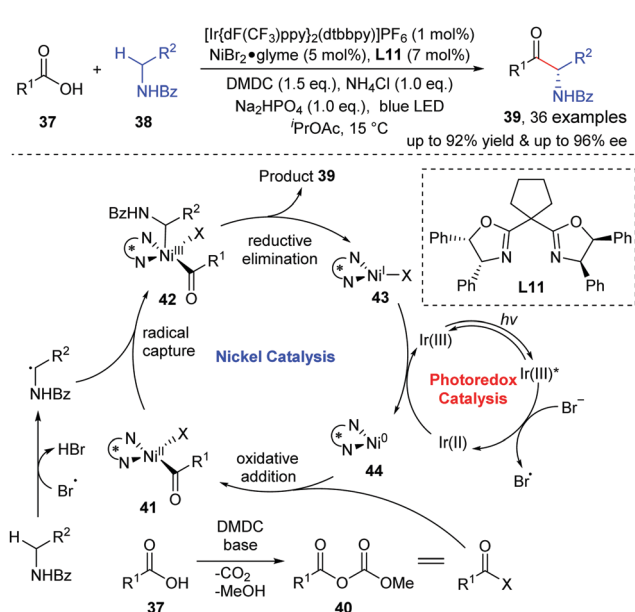
co-workers constructed a chiral centre at the α -position of the carbonyl group by combining the excited state chemistry of HEH with chiral nickel catalysis (Scheme 13).⁴⁰ The excited HEH can not only act as a radical precursor but also act as a reagent to reduce Ni, thereby avoiding the use of photocatalysts. A variety of readily available anhydrides are used in the reaction as the acyl source, and benzyl HEHs can be used in this reaction under the irradiation of 405 nm light.

Recently, Wang and co-workers successfully achieved an efficient synthesis of diverse chiral 3,3-disubstituted oxindoles **36** through the combination of photocatalysis with asymmetric nickel catalysis (Scheme 14).⁴¹ Carbamoyl chlorides **34** and alkyl aldehydes **35** were selected as coupling reagents, and efficient coupling reactions were realized in the presence of a chiral nickel catalyst, tetrabutylammonium decatungstate (TBADT), under 390 nm radiation. After experiments to verify the mechanism, such as experiments with equivalent metals, the following plausible reaction mechanisms were proposed. Initially, TBADT ($[W]^{4-}$) reaches the excited state ($[W]^{4-\bullet}$) under irradiation and then abstracts a hydrogen atom from the aldehyde to form an acyl radical and $[W]^{5-H^+}$. Then, disproportionation takes place between the two $[W]^{5-H^+}$ ions to form $[W]^{6-2H^+}$ and regenerate the ground-state $[W]^{4-}$. Alternatively, the Ni(0) species capture the acyl radical to form acyl Ni(I) species, which then undergoes an oxidative addition with carbamoyl chloride to afford acyl Ni(III) species. After intramolecular enantio-determining migration insertion, a chiral Ni(III) intermediate is formed. Finally, the reductive elimination of the Ni(III) intermediate gives the final chiral oxindole product and Ni(I) species, which is then reduced by $[W]^{6-2H^+}$ to close the catalytic cycle.



Scheme 14 Photoredox/nickel-catalysed asymmetric acyl-carbamoylation of alkenes.

Huo *et al.* also applied the combination of nickel catalysis and the HAT process to construct chiral α -aminoketones **39** (Scheme 15).⁴² Different from traditional electrophilic amination and nucleophilic amination reactions at the α -position of the carbonyl group, this methodology avoids the use of diazoketones and azodicarboxylates and can give chiral α -aminoketones with high efficiency and enantioselectivity starting from simple carboxylic acids and amines. By reacting with dimethyl dicarbonate (DMDC), carboxylic acids **37** can be *in situ* converted to mixed anhydrides **40**, and the latter can undergo oxidative addition with Ni(0) species to form Ni(II) species **41**. At the same time, the

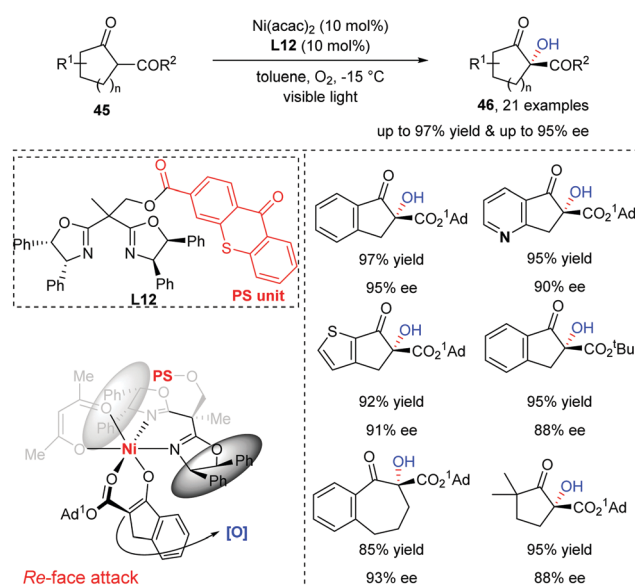


Scheme 15 Photoredox/nickel-catalysed enantioselective C(sp³)-H acylation.

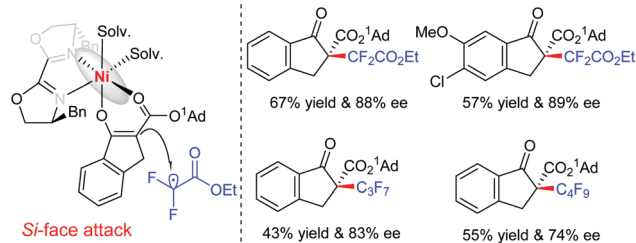
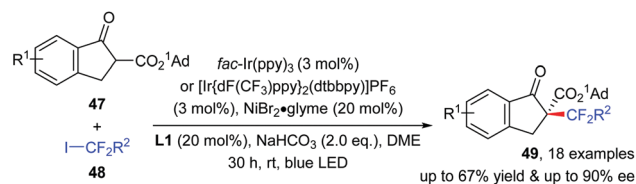
bromine radical produced under photoredox conditions undergoes HAT to generate stable α -amino radical species. These radical species are then captured by Ni(II) in a stereoselective manner to form Ni(III) species **42**. The target product can be obtained by the reductive elimination of **42**, and the resulting Ni(I) species can be reduced by the reduced photocatalyst to regenerate the Ni(0) species and close both catalytic cycles. This photoredox and transition metal catalysis strategy undoubtedly provides a new way to asymmetrically functionalize alkyl C-H bonds.

In 2017, Xiao *et al.* designed and synthesized a class of light-responsive chiral oxazoline ligands, which can be *in situ* converted to bifunctional photocatalysts by coordinating with nickel salts. The formed chiral nickel complexes can be used to catalyse the asymmetric aerobic oxidation of β -ketoesters **45** leading to chiral alcohols **46** in generally high yields and enantioselectivities (Scheme 16).⁴³ Compared with traditional asymmetric oxidation reactions, this reaction uses oxygen as the oxidant to ensure green and safe reaction conditions and does not require the use of highly active oxidants. Notably, the photosensitive ketone fragment in these bifunctional catalysts is used to generate single-state oxygen under irradiation of visible light, even the sunlight, and the chiral oxazoline fragment functions as the key element to induce the enantioselectivity. Based on the properties of the nickel(II) complex and previous studies, the authors also proposed a reasonable control model for the stereo-control of the reaction.

Subsequently, a similar photo-nickel catalytic strategy was developed by the same group for the di/trifluoroalkylation of β -ketoesters **47** to construct fluorine-containing chiral compounds (Scheme 17).⁴⁴ To meet the redox potential requirements, additional Ir catalysts are used in the reaction system, and chiral oxazoline ligands are employed to induce the stereoselectivity of the reaction. Different from the above asymmetric aerobic oxidation reaction, high enantioselectivity in this reaction can only be observed when benzocyclopentanones are used for unknown reasons.



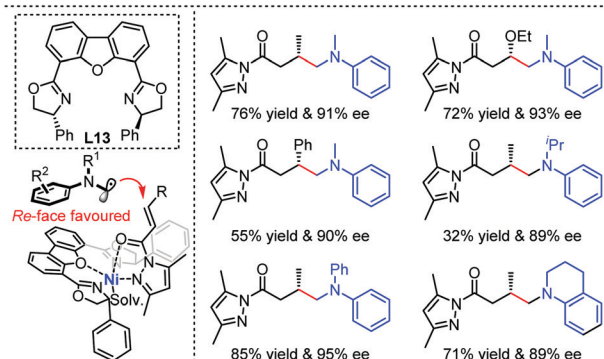
Scheme 16 Photoredox/nickel-catalysed enantioselective aerobic oxidation of β -ketoesters.



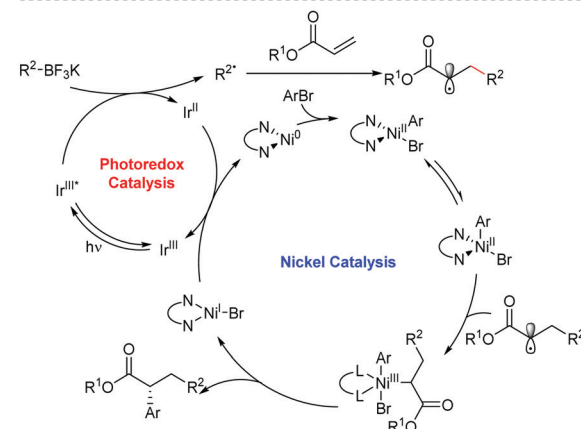
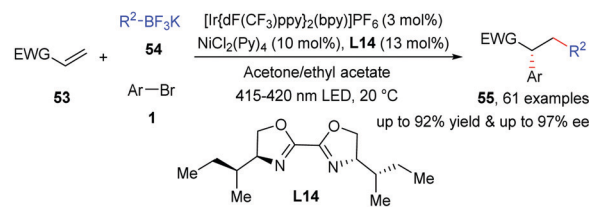
Scheme 17 Photoredox/nickel-catalysed enantioselective di-/perfluoroalkylation of β -ketoesters.

In 2018, Gong *et al.* used a Ni(II)-DBFOX complex as the bifunctional catalyst to realize the asymmetric free radical conjugate addition, where the nickel complex is used as both a photosensitizer and a chiral Lewis acid to achieve excellent stereo-control (Scheme 18).⁴⁵ A series of chiral γ -amino carboxylic acids and γ -lactam derivatives **52** were obtained in high yields and enantioselectivities from easily available α,β -unsaturated carbonyls **50** and α -silylamines **51**. At the same time, the authors also proposed a transition state for the radical addition and a reasonable explanation for the stereochemical result of the reaction. Later, Cozzi *et al.* reported an isolated example of allylation of aldehydes by jointly using a chiral nickel catalyst and a Ru-based photocatalyst.⁴⁶

In addition to two-component coupling reactions, photoredox/nickel-catalysed multicomponent processes have been well developed in recent years.^{47–52} However, the asymmetric variants were not reported until very recently. In 2020, Chu *et al.* described an enantioselective three-component carboarylation reaction between electron-deficient alkenes **53** and tertiary/secondary



Scheme 18 Enantioselective radical conjugate addition reactions via photoinduced nickel catalysis.

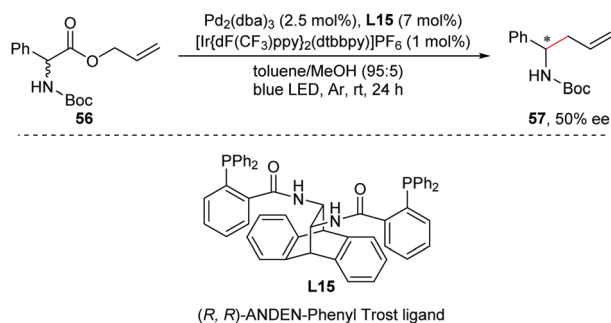


Scheme 19 Photoredox/nickel-catalysed asymmetric three-component carboarylation of alkenes.

alkyl trifluoroborates **54** and aryl bromides promoted by dual photoredox/nickel catalysis (Scheme 19).⁵³ This redox-neutral synthesis strategy can produce a large number of diverse enantio-enriched β -alkyl- α -arylated carbonyl compounds, phosphonates and sulfones from readily available starting materials in high yields and with excellent enantioselectivities. Oxazoline ligands containing four chiral centres are used to achieve a high level of enantioselectivity control. Based on experimental studies and DFT calculations, a possible reaction mechanism was proposed. First, potassium alkyl fluoroborates are reduced by the excited photocatalysts to obtain alkyl radicals, which are then added to olefins to generate new alkyl radicals. Alternatively, the oxidative addition of Ni(0) by aryl halides results in planar Ni(II) species, which can undergo isomerization and intersystem crossing to form more stable tetrahedral triple spin-state Ni(II) species. Subsequently, the triplet nickel species captures the alkyl radicals and undergoes reductive elimination to deliver the desired product and Ni(I) species. Finally, the reduced-state Ir(II) reduces Ni(I) to Ni(0) and closes the two catalytic cycles. The addition of radicals to the triplet tetrahedral Ni(II) species is the stereo-determining step of the reaction. In the dominant transition state, the van der Waals interactions of the aryl group and the carbonyl group with the alkyl side chain of the chiral ligand were believed to be important to define the enantioselectivity.

3. Photoinduced asymmetric coupling reactions with a chiral palladium catalyst

Palladium is a versatile metal catalyst being widely used for a diverse range of coupling reactions. Among them, palladium-catalysed allylic alkylations have been established as an



Scheme 20 Photoredox/palladium-catalysed asymmetric decarboxylative allylations of α -amino acids.

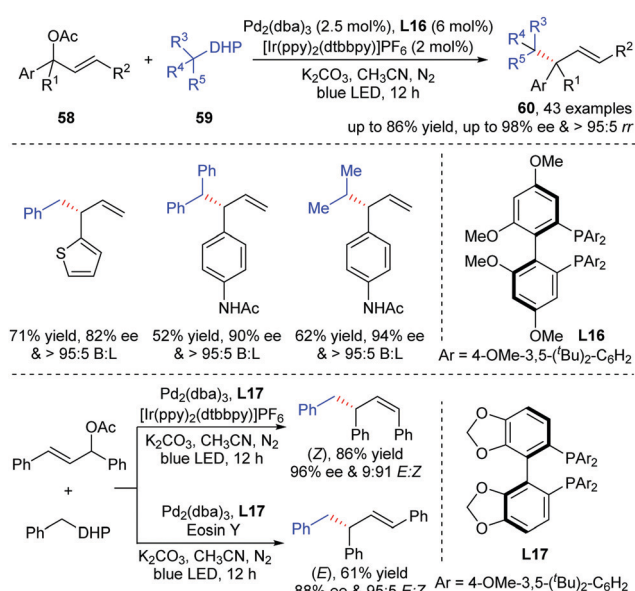
important platform for the construction of chemical bonds. Recently, the dual catalysis strategy merging palladium catalysis with photoredox catalysis enabled the achievement of allylations and related benzylations under very mild conditions, especially the enantioselective processes that are otherwise inaccessible.

Pioneeringly, Tunge *et al.* and Lu, Xiao *et al.* applied this dual strategy to realize the radical allylic alkylation of α -C-H bonds of amines and decarboxylative allylations of amino acid-derived allylic esters independently.^{54,55} One year later, Tunge *et al.* achieved an enantioselective variant with the use of chiral biphenyl phosphine ligand **L15** (Scheme 20).⁵⁶ Modest enantioselectivity was observed (50% ee) when a racemic substrate **56** was used. In 2018, Yu's group utilized this photoredox/palladium dual catalysis strategy to achieve an asymmetric allylic alkylation in the coupling of alkyl radicals stemming from 4-alkyl-1,4-dihydropyridines **59** (Scheme 21).⁵⁷ This reaction system is different from traditional palladium-catalysed asymmetric allylic alkylation in terms of the dynamic kinetic resolution effect and regioselectivity. Under the optimal reaction conditions, branched products were isolated as the sole ones with non-symmetrical monosubstituted allylic

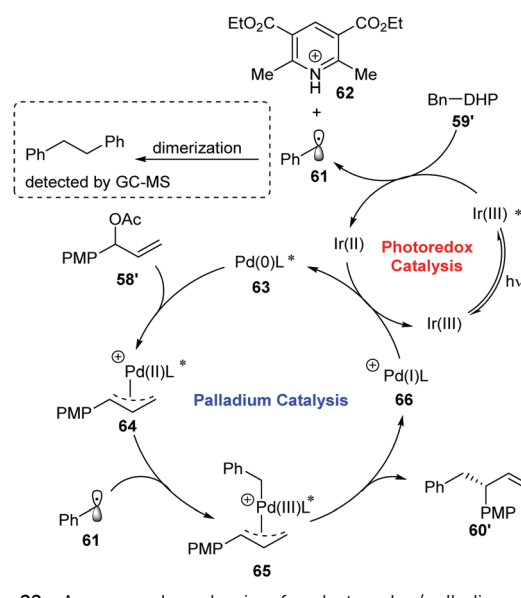
electrophiles. In particular, reactions of primary, secondary and tertiary alkyl radicals with various racemic aromatic allylic acetates, including 1,3-disubstituted unsymmetric allylic esters, generated the desired products with good regio-, enantio-, and *E/Z* selectivities. Moreover, the configuration of alkene products can be controlled by choosing suitable photocatalysts. Although representing an important advance, the same transformation with aliphatic allylic acetates is still under-developed.

Furthermore, the authors proposed a possible mechanism to illustrate the above transformation (Scheme 22). The reaction starts from SET-based oxidation of dihydropyridine **59** by excited-state Ir(III)* to give alkyl radical **61**, low-valent Ir(II) and side product **62**. The radical dimerization detected by GC-MS proves the presence of alkyl radical **61**. Alternatively, an oxidative addition of Pd(0) by allyl esters **56** gives Pd(II)- π -allyl species **64**. Subsequently, Pd(II)- π -allyl species **64** capture alkyl radicals **61** to generate Pd(III) complexes **65**, which undergo reductive elimination to give the products and generate Pd(I) species **66**. Finally, the Ir(II) complexes reduce the Pd(I) species **66** to Pd(0) **63** with regeneration of ground-state Ir(III), thereby closing both catalytic cycles.

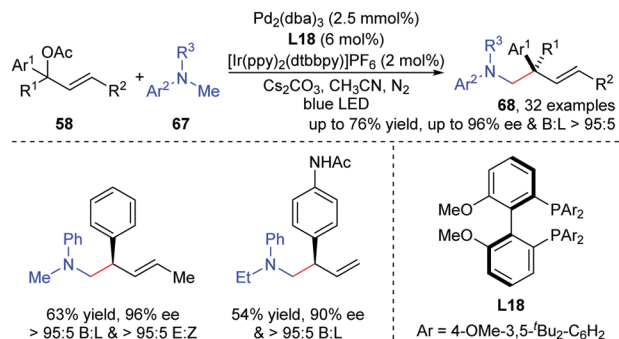
Following a similar catalytic principle, in 2020 Yu's group proved the feasibility of an enantio- and branch-selective α -allylation procedure with another class of radical precursors, namely, *N*-methyl anilines (Scheme 23).⁵⁸ Commercially available *N*-methyl anilines **67**, which do not require preactivation, were employed in lieu of 4-alkyl-1,4-dihydropyridines as formal "hard" alkyl nucleophiles. The only by-product is acetic acid, reflecting a good atom economy of this reaction. A wide array of chiral homoallylic amines, including **68** with an all-carbon quaternary stereogenic centre, were synthesized efficiently with high enantioselectivity. When *N*-methyl-*N*-alkylanilines were used as radical precursors, the methyl moieties were allylated exclusively.



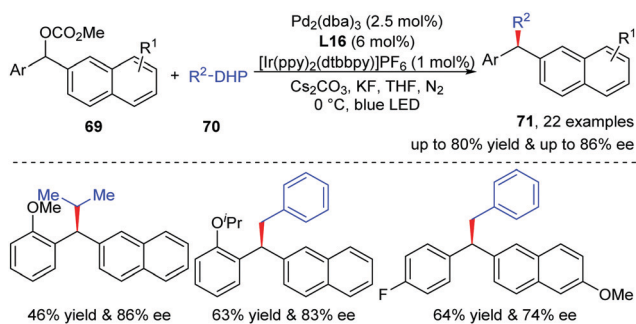
Scheme 21 Photoredox/palladium-catalysed asymmetric allylic alkylation.



Scheme 22 A proposed mechanism for photoredox/palladium-catalysed asymmetric allylic alkylation.



Scheme 23 Photoredox/palladium-catalysed enantioselective α -allylation of anilines.



Scheme 24 Photoredox/palladium-catalysed enantioselective alkylation of secondary benzyl carbonates.

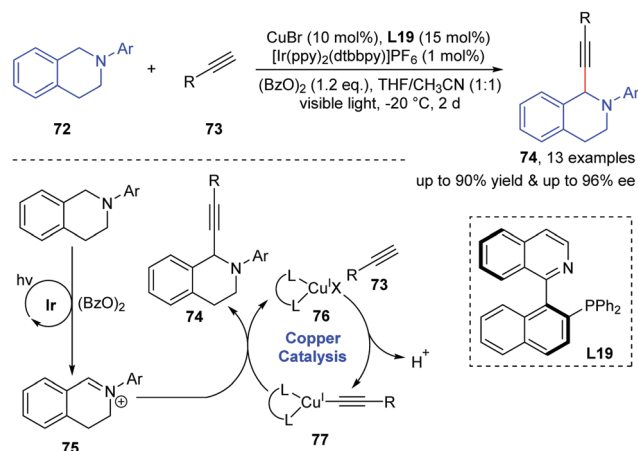
Shortly afterwards, the same group disclosed an asymmetric benzylic substitution reaction through the same catalysis strategy (Scheme 24).⁵⁹ A multifarious set of racemic diarylmethyl carbonates were coupled with 4-alkyl-substituted Hantzsch esters in generally high efficiency and stereoselectivity under redox-neutral conditions.

4. Photoinduced asymmetric coupling reactions with a chiral copper catalyst

4.1 Dual photoredox/copper catalysis

Copper, owing to its low toxicity and cost, is widely used in transition metal catalysis.⁶⁰ As an effective dual catalysis system, the combination of photoredox catalysis with copper catalysis has been investigated extensively. In the past few years, great advances have been made in enantioselective transformations *via* this strategy.

In 2015, Li *et al.* accomplished an asymmetric alkylation of tetrahydroisoquinoline by dual photoredox/copper catalysis with benzoyl peroxide as the terminal oxidant and chiral ligand **L19** as the optical ligand (Scheme 25).⁶¹ Tetrahydroisoquinolines **72** can smoothly react with terminal alkynes **73** to produce 1-alkynyl tetrahydroisoquinolines **74** in moderate to good yields and with high enantioselectivities. Mechanistically, the transformation begins with SET-based oxidation of tetrahydroisoquinoline **72** by the photoexcited Ir(III)* catalyst to generate an amine radical cation and an Ir(II) catalyst. Then, benzoyl peroxide can be reduced

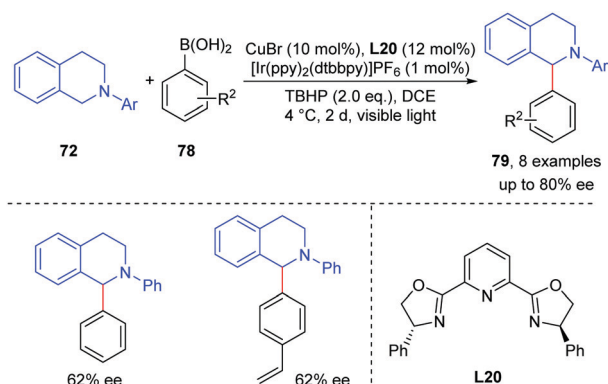


Scheme 25 Photoredox/copper-catalysed asymmetric cross-dehydrogenative coupling of alkynes with tetrahydroisoquinolines.

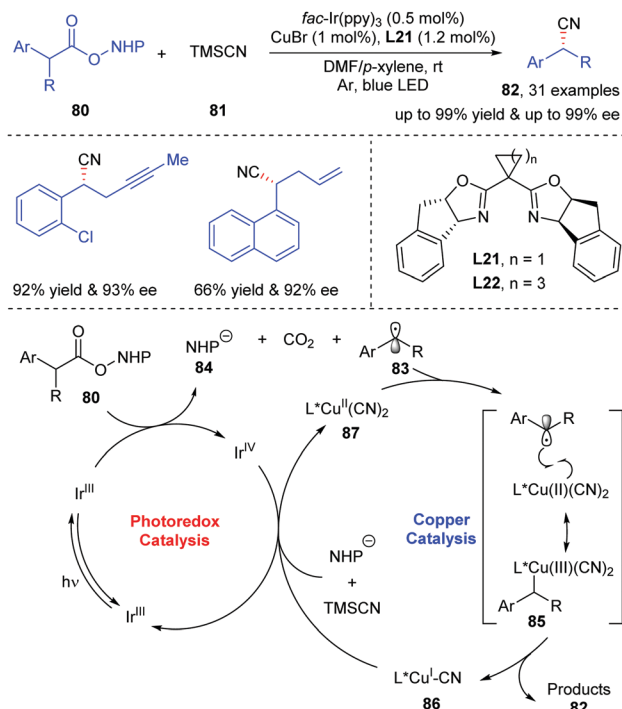
to BzO^- and BzO^\bullet by the strongly reducing Ir(II) catalyst with regeneration of the ground-state Ir(III) catalyst. Alternatively, the amine radical cation can be converted to reactive iminium ion intermediate **75**, which undergoes nucleophilic addition with chiral Cu(I)-acetylide complex **77** to give optically active 1-alkynyl tetrahydroisoquinoline.

Encouraged by this success, in 2016 they further applied this strategy to an asymmetric arylation of *N*-aryl tetrahydroisoquinolines with PhPyBox as the chiral ligand (Scheme 26).⁶² Utilizing aryl boronic acids as nucleophile precursors and TBHP as an oxidant, optically active products **79** were afforded in modest to good enantioselectivities (26–88% ee).

In 2017, Liu and Lin *et al.* probed the feasibility of an asymmetric decarboxylative cyanation of *N*-hydroxy-phthalimide (NHP) esters **80** with trimethylsilyl cyanide (TMSCN) through dual photoredox/copper catalysis (Scheme 27).⁶³ A broad family of enantio-enriched benzyl nitriles, including the key chiral intermediates for bioactive compounds, were efficiently produced by using a chiral bis(oxazoline) (BOX) ligand under mild conditions. Mechanistically, upon irradiation with blue LEDs, the redox-active NHP ester can receive a single electron from photoexcited Ir(III), followed by radical decarboxylation to give benzylic radical **83**.



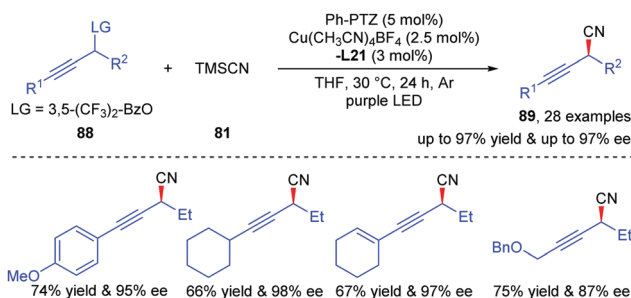
Scheme 26 Photoredox/copper-catalysed asymmetric C(sp³)-H arylation of tetrahydroisoquinolines.



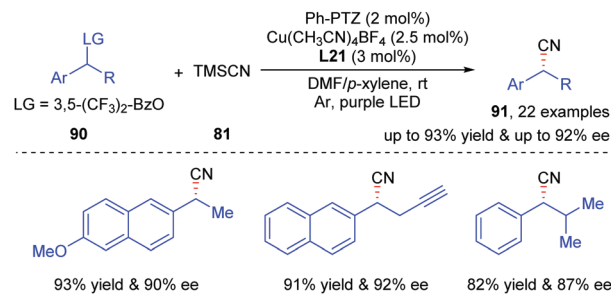
Scheme 27 Photoredox/copper-catalysed enantioselective decarboxylative cyanation and proposed mechanism.

The key to the success is attributed to the reactivity profile of Ir(IV), which can oxidize L*Cu(I)CN species **86** to form L*Cu(II)(CN)₂ species **87** with regeneration of ground-state Ir(III). Prochiral benzylic radical **80** can be captured by L*Cu(II)(CN)₂ species **87**, and reductive elimination finally delivers chiral nitriles **82** and releases L*Cu(I)CN species **86**.

Optically active propargyl cyanides are versatile building blocks in organic chemistry.⁶⁴ In 2019, Lu and Xiao accomplished an asymmetric propargylic radical cyanation of propargyl esters through photoredox/copper dual catalysis, affording a wide range of chiral propargyl cyanides with high yields and stereocontrol (Scheme 28).⁶⁵ In lieu of the expensive *fac*-Ir(ppy)₃, the organic photocatalyst 10-phenylphenothiazine (Ph-PTZ) was applied not only to generate propargyl radicals but also to oxidize Cu(I) species. Additionally, mechanistic experiments and DFT calculations proved that the irreversible reductive elimination of the propargyl-Cu(III) complex determined the stereochemistry. The similar catalytic



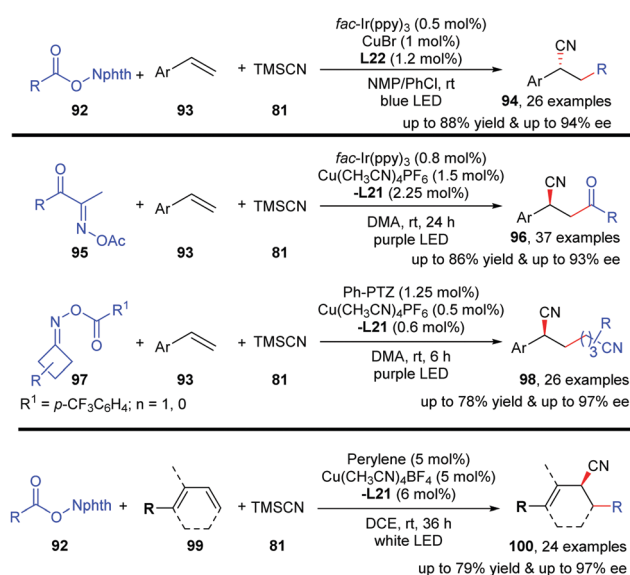
Scheme 28 Photoredox/copper-catalysed asymmetric propargylic radical cyanation.



Scheme 29 Photoredox/copper-catalysed asymmetric deoxygenative cyanation of benzyl alcohols.

system can be further applied to the asymmetric deoxygenative cyanation of readily available benzyl esters (Scheme 29).⁶⁶

Owing to their capacity to facilitate the construction of complex molecules from easily available alkene feedstocks, radical-involved alkene 1,2-difunctionalization has emerged as a promising strategy.⁶⁷ In 2018, Han and Mei disclosed an enantioselective radical cyanoalkylation of styrenes by photoredox/copper dual catalysis, offering an immediate path to various chiral alkyl nitriles (Scheme 30, up).⁶⁸ In this process, the alkyl radicals produced by photoredox reactions from inexpensive and abundant carboxylic acids add to styrene **93** to deliver the key intermediate benzylic radical. This key intermediate couples with an L*Cu(II)CN complex to provide enantioselectively enriched alkylated benzylic nitriles. The scope of radical precursors can be expanded to primary, secondary, and tertiary aliphatic NHP esters, while this transformation is mainly limited to aromatic olefins. Following a similar catalytic principle, in 2021, Chen and Xiao achieved an intermolecular, enantioselective three-component radical vicinal dicarbofunctionalization reaction of olefins under mild conditions with the oxime esters as the radical precursors, leading to valuable optically active β-cyano ketones and alkyl dinitriles, respectively, in a highly enantioselective manner



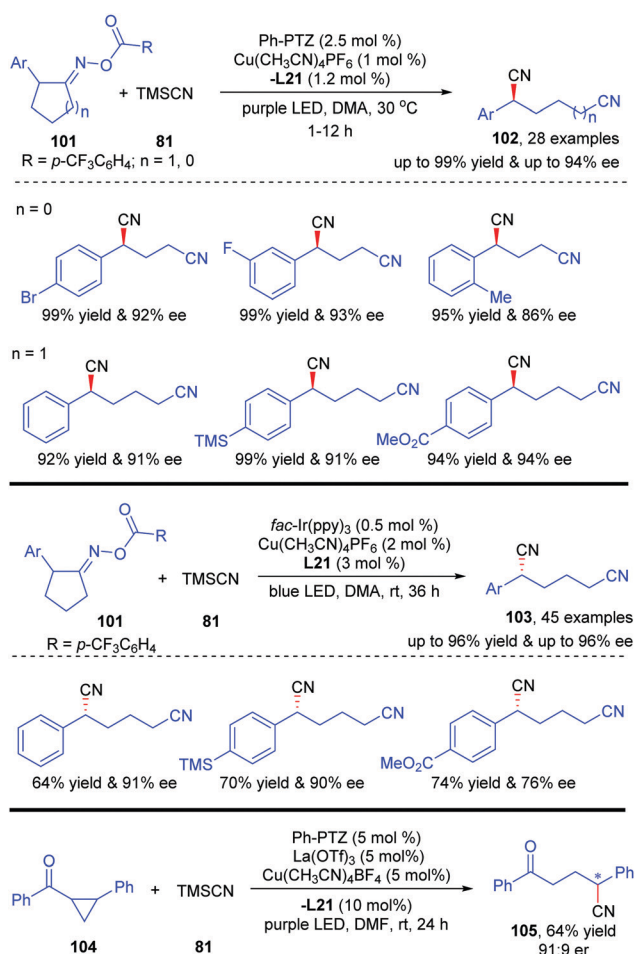
Scheme 30 Photoredox/copper-catalysed asymmetric cyanoalkylation reaction of alkenes.

(Scheme 30, middle).⁶⁹ Meanwhile, Lu and Xiao also realized the enantioselective radical carbocyanation of 1,3-dienes and 1,3-enynes (Scheme 30, down).⁷⁰ Through this protocol, a wide range of chiral allyl cyanides and propargyl cyanides are produced in good yields and high enantioselectivities. At the same time, this strategy further enriches the asymmetric transformation of 1,3-diene in excited state chemistry.

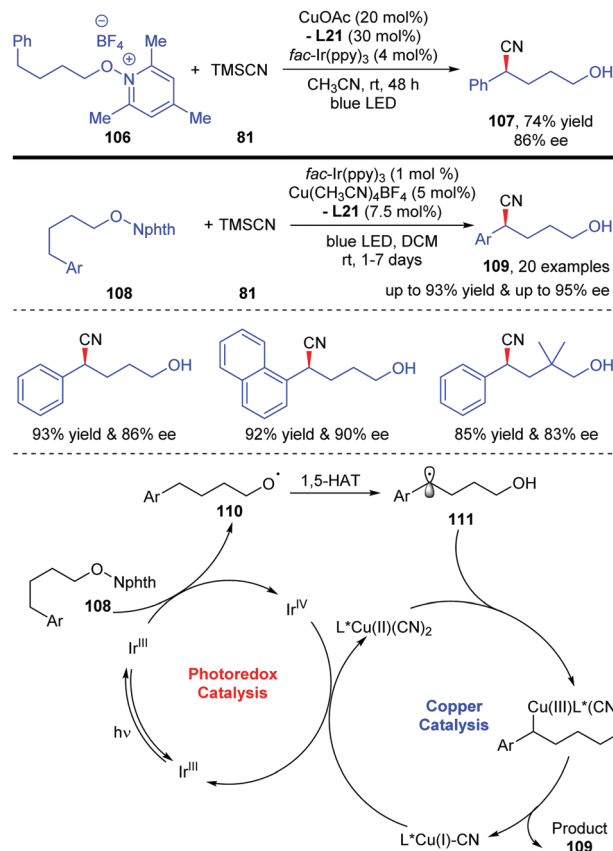
Encouraged by the success of asymmetric control with chiral copper catalysts, the group of Xiao focused on the photocatalytic enantioselective radical cyanation reactions of cycloketone-derived oxime esters and cyclopropyl ketones (Scheme 31). In 2019, Chen and Xiao developed an asymmetric ring-opening cyanation of oxime esters for the assembly of valuable chiral alkyl dinitrile derivatives.⁷¹ The substrate scope is considerably broad and the functional group compatibility is quite good. The same catalysis system was successfully applied to an enantioselective three-component, ring-opening cross coupling when cyclobutanone oxime ester and styrenes were employed in lieu of 2-aryl-substituted cycloketone-derived oxime esters. A similar catalytic strategy was disclosed by Wang's group,⁷² who applied *fac*-Ir(ppy)₃ as the photocatalyst instead of the organic photocatalyst Ph-PTZ. Subsequently, Cheng and Xiao further extended the radical

ring-opening cyanation strategy to cyclopropyl ketones, producing enantio-enriched γ -cyanoketones by merging Lewis acid catalysis, copper catalysis and photoredox catalysis.⁷³ Moderate enantio-induction was observed by using the chiral BOX ligand (Scheme 31, down).

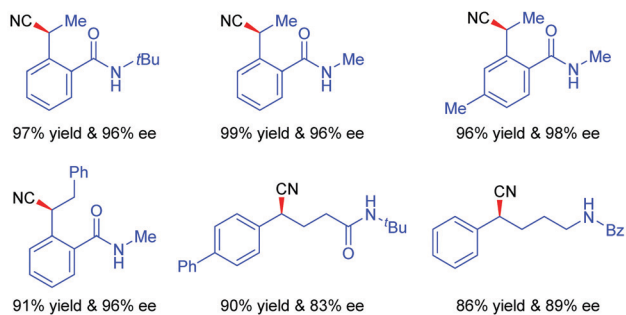
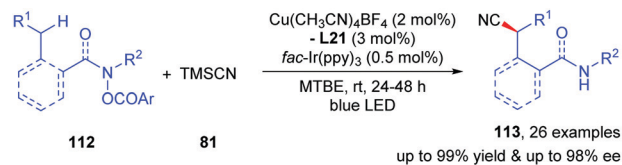
In 2019, the Zhu group⁷⁴ and the Liu group⁷⁵ independently developed an enantioselective cyanation of remote C(sp³)-H bonds by dual photoredox and copper catalysis (Scheme 32). The Zhu group utilized *N*-alkoxy-pyridinium salts **106** as the radical precursors, whereas *N*-alkoxyphthalimides **108** were used by the Liu group. Analogously, there was a SET between the radical precursor *N*-alkoxy-pyridinium salts **106** or *N*-alkoxyphthalimides **108** and photoexcited Ir(III)* generated alkoxy radical **110**. The benzylic radical **111** derived from the 1,5-HAT of alkoxy radical **110** would be trapped by L^{*}Cu(II)(CN)₂ to afford chiral Cu(III) species. A final reductive elimination step produced the desired products **109** while regenerating the chiral Cu(I) species. Zhu's group also demonstrated that δ -azido, δ -cyano, and δ -thiocyanato alcohols were produced in high yields when 1,10-Phen was used as the ligand instead of the chiral ligand L21. Liu's group proved that δ -cyano alcohol can be converted to amino alcohol in good yield without a distinct decrease in the ee value. Following a similar mechanistic principle, in 2020 the Yu group developed a *N*-radical-mediated, enantioselective benzyl C-H cyanation of *O*-acyl hydroxamides (Scheme 33).⁷⁶



Scheme 31 Photoredox/copper-catalysed enantioselective radical ring-opening cyanation.



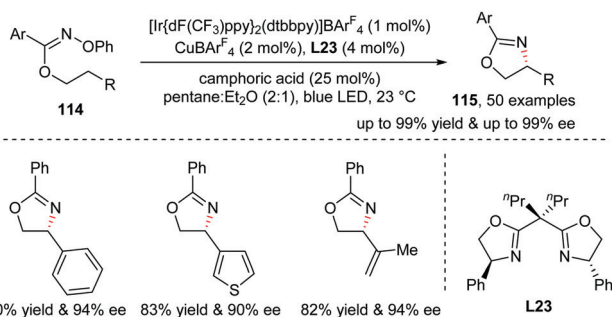
Scheme 32 Photoredox/copper-catalysed asymmetric cyanation of remote C-H bonds.



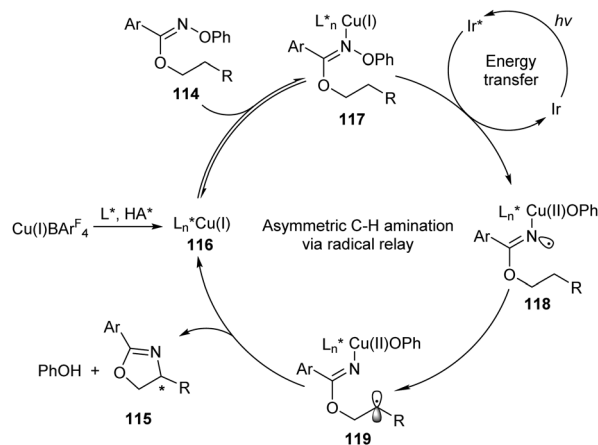
Scheme 33 *N*-Radical-mediated enantioselective benzyl C–H cyanation of *O*-acyl hydroxamides.

In 2019, Nagib's group developed an enantio- and regioselective radical $\text{C}(\text{sp}^3)\text{-H}$ amination for the synthesis of optically active β -amino alcohols from achiral oxime imidates (Scheme 34).⁷⁷ Importantly, this dual catalysis system is not limited to benzylic $\text{C}(\text{sp}^3)\text{-H}$ amination and the oxime imidates derived from allylic, propargylic and aliphatic alcohols are also suitable. A variety of chiral oxazoline products were formed with excellent functional group tolerance, reaction efficiencies and enantioselectivities. Notably, the chiral oxazoline products can be converted to an array of valuable chiral amino alcohols by cleavage of the heterocycles. Mechanistic studies indicated that the $\text{Cu}(\text{i})$ -coordinated imidate intermediate can accept the energy from the triplet-state photocatalyst.

To illustrate this coupling reaction, a plausible mechanism was proposed as displayed in Scheme 35. First, chiral $\text{Cu}(\text{i})$ catalyst **116** coordinates with radical precursor **114** to produce $\text{Cu}(\text{i})$ imidate complex **117**. Then, through an energy transfer mechanism, photoexcited $\text{Ir}(\text{iii})^*$ sensitizes the chiral organocopper complex and generates *N*-centred radical **118**. The resulting chiral $\text{Cu}(\text{ii})$ -bound imidate radical **118** undergoes an enantio- and regioselective HAT process to generate chiral β -radical **119**. Finally, chiral β -radical **119** undergoes a stereoselective amination to give



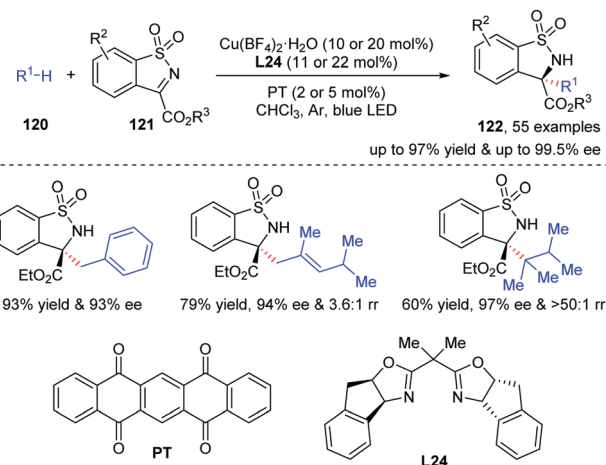
Scheme 34 Photoredox/copper-catalysed enantioselective radical C–H amination of remote C–H bonds.



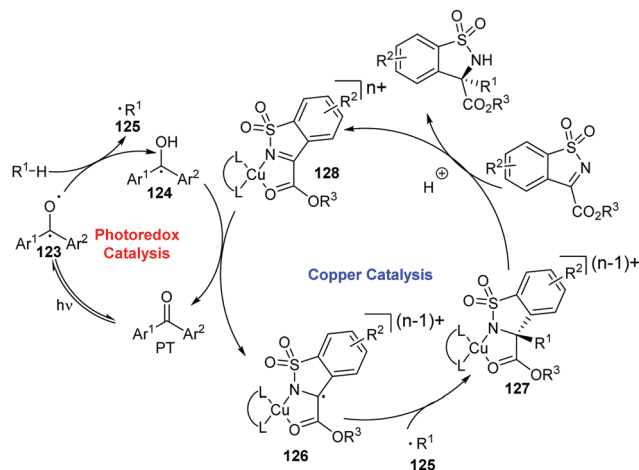
Scheme 35 A proposed mechanism of photoredox/copper-catalysed enantioselective radical C–H amination of remote C–H bonds.

enantioenriched oxazoline **115**, along with PhOH and regenerated chiral $\text{Cu}(\text{i})$ catalyst **116**, closing the catalytic cycle.

In 2019, the Gong group reported a highly regio- and stereoselective $\text{C}(\text{sp}^3)\text{-H}$ functionalization of alkanes with *N*-sulfonylimines by utilizing a HAT photocatalyst and a chiral copper catalyst under mild conditions (Scheme 36).⁷⁸ The dual catalysis system enables precise site recognition and enantioselective induction of the unactivated $\text{C}(\text{sp}^3)\text{-H}$ bonds. As a result, benzylic and allylic hydrocarbons and even alkanes can be transformed to chiral products with good to excellent reaction efficiencies and high regio- and stereoselectivities (up to >50:1 r.r. and 99.5% ee). Notably, tertiary benzylic radicals were also suitable for this transformation, accompanied by excellent stereocontrol (>90% ee). A possible mechanism is shown in Scheme 37. The reaction begins with hydrogen atom abstraction from **120** to give semiquinone-type radical **124** and alkyl radical **125** via a long-lived triplet state, biradical species **123**, upon irradiation with blue LEDs. The authors speculated that an obvious difference in the rate of $\text{C}(\text{sp}^3)\text{-H}$ bond activation depended on both the steric hindrance of the HAT photocatalyst



Scheme 36 Photoredox/copper-catalysed regio- and enantioselective $\text{C}(\text{sp}^3)\text{-H}$ functionalization.

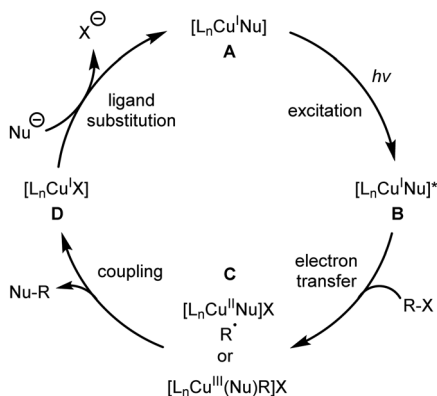


Scheme 37 A proposed mechanism of photoredox/copper-catalysed regio- and stereoselective C(sp³)-H functionalization of benzylic and allylic hydrocarbons.

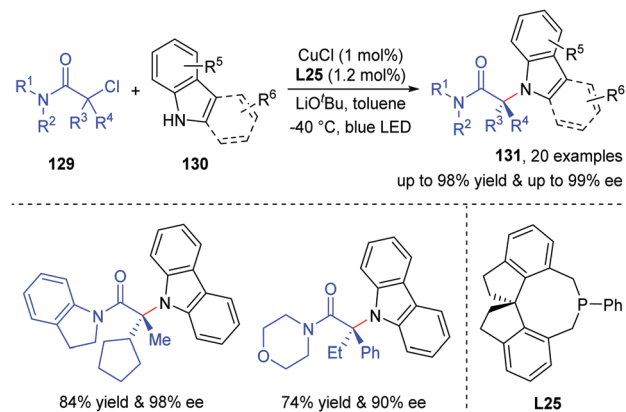
and the inherent stability of the produced alkyl radicals **125**. The imine substrate is then coordinated by a chiral metal catalyst to form complex **128**, followed by SET with semiquinone-type radical **124** to deliver metal-stabilized carbon radical **126** with regeneration of ground-state PT. Intermediate **127** was generated *via* the cross-coupling of radical **125** with the persistent radical **126**, in which the chiral ligand-transition-metal moiety sterically governs the regio- and stereoselectivity. Finally, intermediate **127** undergoes a protonation and a ligand substitution to give the chiral product with regeneration of coordinated imine.

4.2 Bifunctional copper catalysis

Different from the aforementioned examples with an additional photocatalyst, the use of chiral copper-nucleophile complexes as bifunctional catalysts in the photoinduced asymmetric couplings has also been developed.⁷⁹ A general mechanism is depicted in Scheme 38. First, the *in situ* generated copper-nucleophile can absorb visible light and serve as a photoredox agent. A radical precursor is oxidized by the excited-state copper-nucleophile complex to give the radicals, which can be captured by the copper-nucleophile complex. Finally, the formed Cu(III) species undergo a reductive elimination to deliver the chiral product.



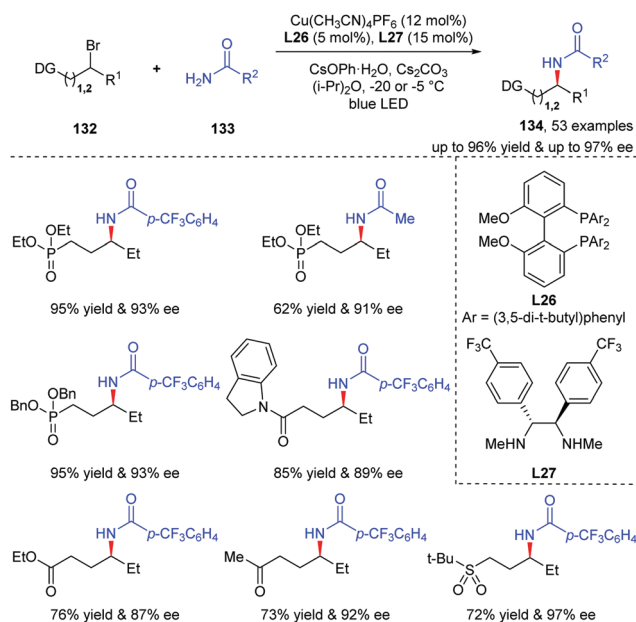
Scheme 38 A general mechanism for bifunctional copper catalysis.



Scheme 39 Photoinduced copper-catalysed asymmetric C-N cross-couplings.

In 2016, Fu and Peters *et al.* realized a copper-catalysed photoredox asymmetric C-N cross-coupling of amines using racemic tertiary alkyl chloride electrophiles **129** as radical precursors to produce fully substituted stereocentres with high enantiocontrol under irradiation using a blue LED (Scheme 39).⁸⁰ In this work, the chiral copper-nucleophile complex served not only as a photoredox catalyst to engage in SET with an alkyl halide to deliver an alkyl radical, but also as a chiral catalyst for C-N bond formation. Carbazoles, C3-substituted indoles and a variety of tertiary alkyl halides work well in the photoinduced copper catalysis system.

In 2021, Fu and Peters *et al.* developed a new, convergent method for the asymmetric synthesis of secondary amides starting from unactivated alkyl electrophiles and nitrogen nucleophiles (specifically, primary amides) by photoinduced copper catalysis, which expands the range of alkyl electrophilicity (Scheme 40).⁸¹ The key to the success relies upon three classes of ligands that assemble two distinct catalysts *in situ*:



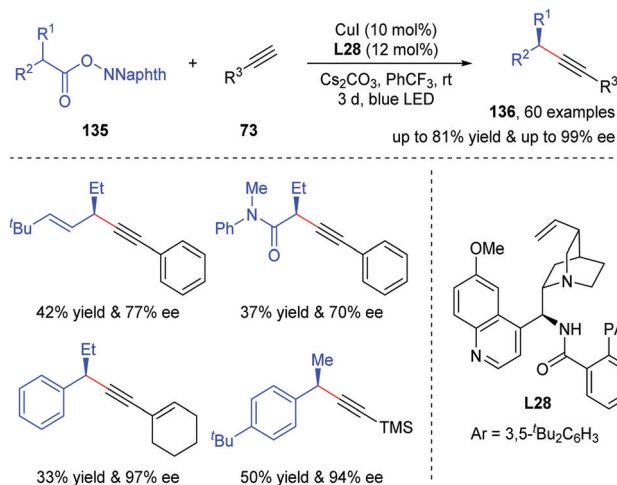
Scheme 40 Photoinduced copper-catalysed asymmetric amidation.

a copper/bisphosphine/phenoxide complex that serves as a photocatalyst to activate the unactivated electrophile, and a chiral copper/diamine complex that achieves enantioselective C–N bond formation.

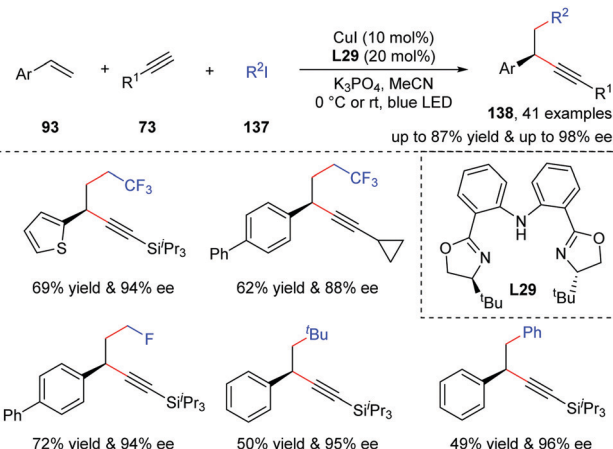
As part of their continuous interest in copper-catalyzed asymmetric radical reactions, Liu and co-workers have designed a novel class of chiral anionic multidentate N,N,P-ligands. This kind of ligands could not only enhance the reducing capability of the copper catalyst to initiate the radical reactions from the relatively inert alkyl halides, but also achieve enantiocontrol over the prochiral alkyl radicals. Thus, they have achieved asymmetric radical transformations with terminal alkynes *via* a copper acetylide intermediate using this chiral copper catalysis.^{82,83} The *in situ*-generated Cu(I) acetylide can also absorb visible light and generate a long-lived excited state and can be used as a reducing agent. In 2020, Liu and co-workers reported a photo-induced, copper-catalysed asymmetric radical decarboxylative alkylation of NHP esters with terminal alkynes (Scheme 41).⁸⁴ Low reaction efficiencies were observed without visible light. In sharp contrast to the previously reported protocol that utilized alkyl halides, the substrate scope was greatly expanded by employing NHP-type esters as the radical precursors. Notably, a chiral cinchona alkaloid-derived N,N,P-ligand was crucial for this catalytic asymmetric alkylation in terms of high yield and enantiocontrol.

In 2020, Zhang and co-workers disclosed an enantioselective radical 1,2-carboalkynylation of alkenes *via* photoinduced copper catalysis, leading to chiral alkynes in high efficiency and enantioselectivity (Scheme 42).⁸⁵ The key to this success is the use of the appropriate chiral Cu(I)-acetylide complex as both the photocatalyst and chiral catalyst. With ^tBu-BOPA (bisoxazoline diphenylamine) as the chiral ligand that was developed by them, the reaction features a broad substrate scope covering (hetero)aryl-substituted alkenes, fluorinated or non-fluorinated alkyl and heteroaryl iodides and (hetero)aryl, alkyl and silyl alkynes.

This strategy can still work very well when employing azoles as the nucleophiles instead of terminal alkynes. Following the



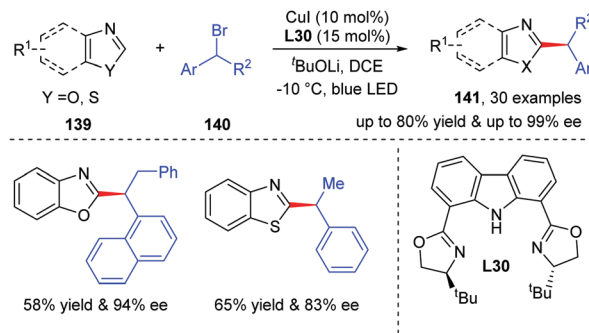
Scheme 41 Photoinduced copper-catalysed asymmetric decarboxylative alkylation of terminal alkynes.



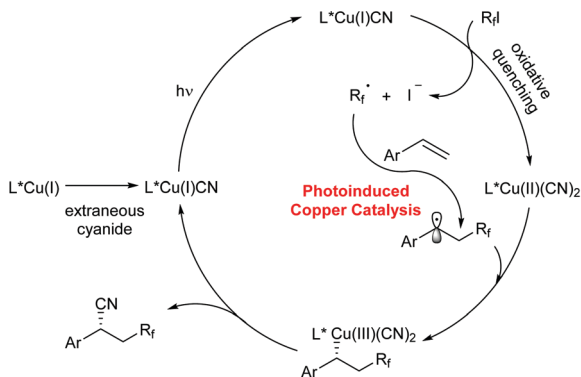
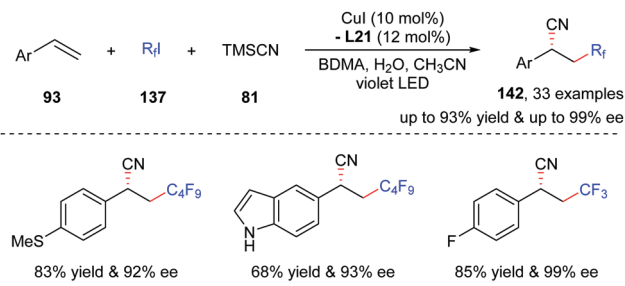
Scheme 42 Photoinduced copper-catalysed asymmetric alkene difunctionalization.

same mechanistic elements, in 2020, the Zhang group proposed a strategy for catalytic enantioselective alkylation of azoles with benzyl bromides employing asymmetric/photoredox bifunctional catalysts based on chiral copper-azole complexes (Scheme 43).⁸⁶ Under visible-light irradiation, the racemic alkyl bromides can be reduced by the excited-state chiral copper-azole complex to give the alkyl radicals and participate in cross-coupling with a broad range of azoles. With ^tBuCbzBox as the chiral ligand, an array of chiral azole products were afforded with good reaction efficiencies and high stereoselectivities.

In 2019, Xu and Wang reported a photoinduced, copper-catalysed asymmetric cyanofluoroalkylation of styrenes with fluorinated alkyl halides as the fluoroalkylation reagents, affording β -fluoroalkylated benzylic nitriles in high yields and enantioselectivities (Scheme 44).⁸⁷ Based on mechanistic investigations, the authors proposed that the *in situ* generated $L^*Cu(I)CN$ species can reach its excited-state $[L^*Cu(I)CN]^*$ under irradiation with violet LEDs. Oxidative quenching of $[L^*Cu(I)CN]^*$ by a fluoroalkyl iodide generates an R_f radical and $L^*Cu(II)(CN)_2$. Subsequently, the R_f radical adds to the alkene to generate the key benzylic radical, which can be trapped by $L^*Cu(II)(CN)_2$ and release the final product through a reductive elimination.

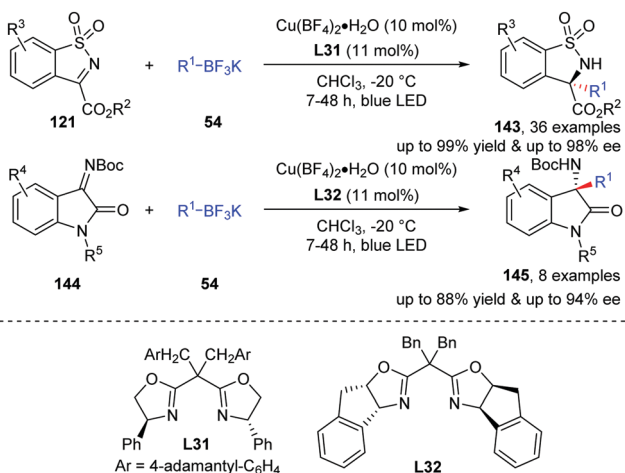


Scheme 43 Photoinduced copper-catalysed asymmetric alkylation of azoles.

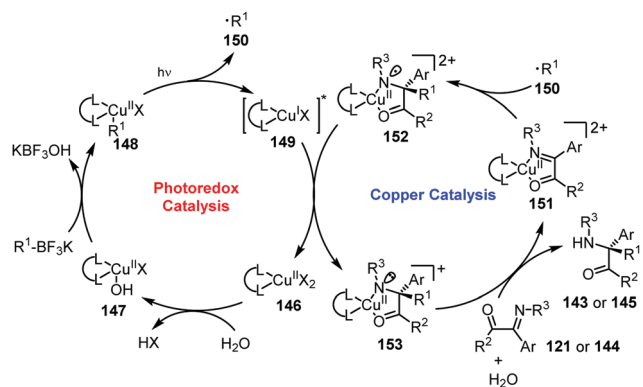


Scheme 44 Asymmetric cyanofluoroalkylation of alkenes via photoinduced copper catalysis.

Different from the reactions depicted above that require suitable nucleophiles to coordinate with copper to form bifunctional photocatalysts, chiral Cu(II)/bisoxazoline [Cu(II)-BOX] complexes themselves can absorb visible light and serve as bifunctional photocatalysts. In 2019, Gong and co-workers proposed a strategy for asymmetric radical addition to activated imines with benzyl trifluoroborate as the radical precursor through photoinduced copper catalysis (Scheme 45).⁸⁸ Both *N*-sulfonylimines and isatin-derived ketimines can be used as efficient radical acceptors, enabling the construction of chiral amines with good to excellent enantiocontrol. A possible reaction mechanism is described in Scheme 46. The reaction begins with ligand exchange between



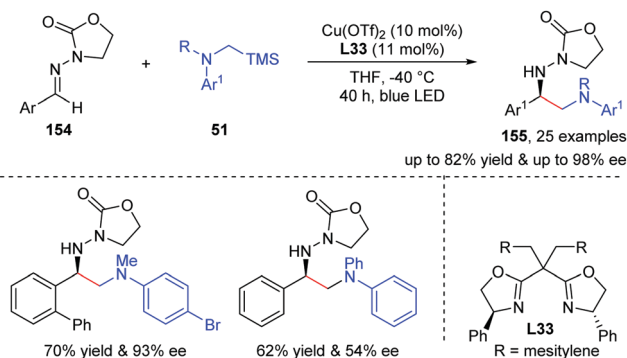
Scheme 45 Asymmetric alkylation of imines via photoinduced copper catalysis.



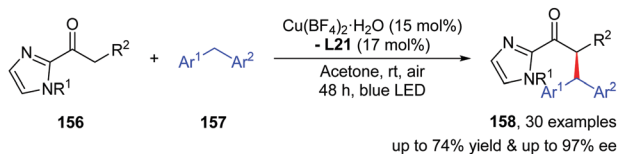
Scheme 46 A proposed mechanism of photoinduced copper-catalysed asymmetric alkylation of imines.

the chiral copper catalyst and alkyl trifluoroborate, followed by light-induced homolysis to generate alkyl radical **150** and Cu(I) species **149**. Meanwhile, another chiral copper that acts as a Lewis acid can coordinate with the imine substrate *via* fast ligand exchange to produce intermediate complex **151**. Nucleophilic alkyl radical **150** attacks the C=N double bond of complex **151** in an enantioselective fashion to give N radical species **152**, which is stabilized by chiral Cu(II). Excited chiral Cu(I) species **149** can reduce intermediate **152** to mono-cationic complex **153** with regeneration of the L*Cu(II) catalyst **146**. Finally, intermediate **153** undergoes protonation and ligand exchange to deliver the chiral product and regenerate intermediate complex **151**.

In 2019, Gong *et al.* further applied the same catalytic strategy to the asymmetric aminoalkylation of acyclic imine derivatives with α -silylamines as the α -aminoalkyl radical precursors (Scheme 47).⁸⁹ The combination of Cu(OTf)₂ and **L33** was the optical choice and a variety of chiral 1,2-diamines were produced in high yield and high enantioselectivity. Meanwhile, the same group developed a visible light-induced, enantioselective aerobic cross-dehydrogenative coupling (CDC) of carbonyl compounds with xanthene by using a chiral copper catalyst. A series of chiral products are furnished with good to excellent yields and high level of enantiocontrol (Scheme 48).⁹⁰ Mechanistic investigations revealed that the copper catalyst exhibited good performance on both photoactivation to initiate the CDC reaction



Scheme 47 Enantioselective α -aminoalkylation *via* photoinduced copper catalysis.



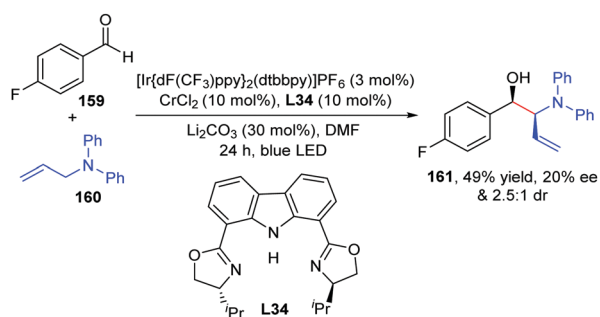
Scheme 48 Asymmetric aerobic cross-dehydrogenative coupling of C(sp³)-H bonds *via* photoinduced asymmetric copper catalysis.

with molecular oxygen and asymmetric induction. This work proves that photoinduced asymmetric copper catalysis can be successfully expanded to difficult asymmetric photochemical reactions.

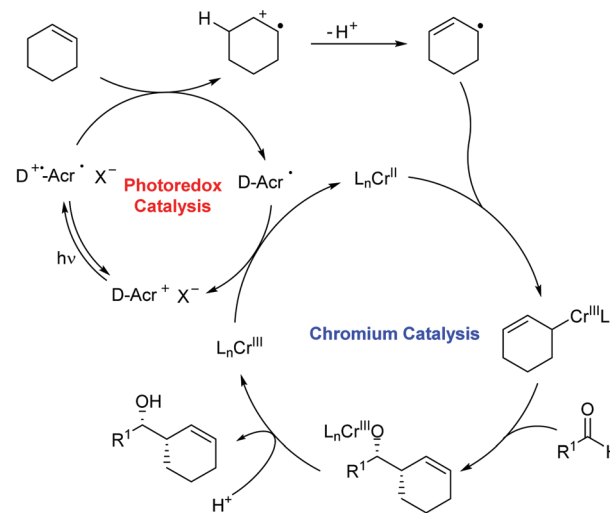
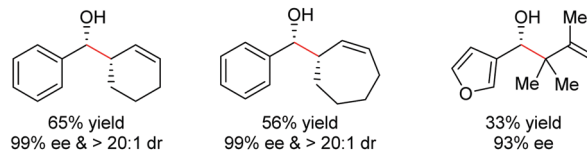
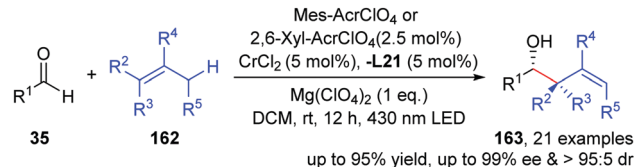
5. Photoinduced asymmetric coupling reactions with chiral chromium catalysts

In addition to asymmetric nickel, palladium and copper catalysis, asymmetric chromium catalysis can be also applied to metallaphotoredox-catalysed coupling reactions, particularly for the asymmetric Nozaki-Hiyama-Kishi (NHK) reaction. In 2018, Glorius *et al.* realized a diastereoselective allylation of aldehydes through a dual photoredox/chromium catalysis strategy, leading to high allyl alcohols generally in high yields and diastereoselectivities.⁹¹ The authors also tested the asymmetric variant by using chiral ligand **L34** (Scheme 49). Although only low enantioselectivity and diastereoselectivity values were observed, it verified the feasibility of the synthesis of chiral homoallyl alcohol through this strategy.

In the same year, Kanai *et al.* accomplished an asymmetric allylation of olefins through the direct C(sp³)-H functionalization of olefins by dual photoredox and chromium catalysis (Scheme 50).⁹² Under the control of the chiral Cr/L complex, a variety of chiral homoallyl alcohols **163** are obtained with high enantioselectivity and diastereoselectivity. Initially, the olefin **162** is oxidized by the excited-state photocatalyst to form a radical cation and then loses a proton to afford allyl radicals. Subsequently, the allyl radical is captured by a chiral Cr(II) catalyst to obtain a Cr(III) species, which then nucleophilically attacks the aldehydes and undergoes protonation to obtain the final homoallyl alcohol products **163** and Cr(III) species. Finally, the reduced photocatalyst reduces Cr(III) to Cr(II) and closes the catalytic cycle. The high diastereoselectivity of this type of



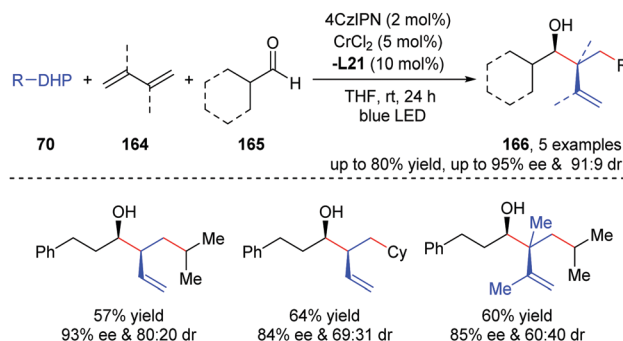
Scheme 49 Photoredox/chromium-catalysed asymmetric allylation of aldehydes.



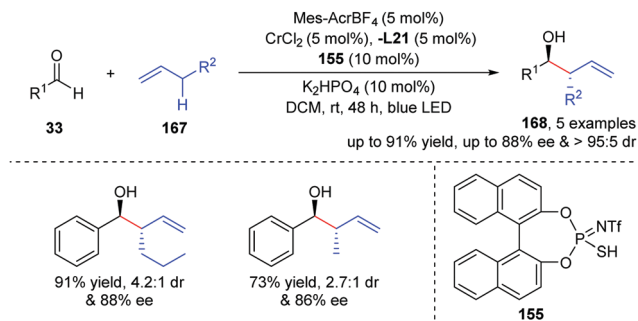
Scheme 50 Photoredox/chromium-catalysed asymmetric allylation of aldehydes.

reaction is mainly due to the Zimmerman-Traxler transition state consisting of chiral allyl chromium and aldehydes.

In 2020, Glorius *et al.* realized a three-component NHK reaction between alkyl-substituted Hantzsch esters, 1,3-dienes and aldehydes enabled by dual photoredox and chromium catalysis (Scheme 51).⁹³ Allyl radicals are formed by addition to 1,3-butadienes with alkyl radicals that are generated from HEHs. This protocol provides a promising route to access value-added chiral homoallylic alcohols from inexpensive and easily available industrial raw materials.



Scheme 51 Photoredox/chromium-catalysed asymmetric dialkylation of 1,3-dienes.



Scheme 52 Photoredox/chromium-catalysed asymmetric allylation of aldehydes using unactivated alkenes.

The asymmetric NHK reaction with unactivated olefins is highly significant, but still very challenging. Until very recently, Kanai *et al.* addressed this problem by combining photoredox-mediated HAT catalysis with asymmetric chromium catalysis (Scheme 52).⁹⁴ The authors skilfully use the sulfur radicals, which are *in situ* generated from thiophosphorimide *via* photoredox catalysis, to grab hydrogen atoms at the allyl position. Thereby, chiral homoallylic alcohols were produced in high yields and good enantioselectivities from readily available olefins and aldehydes. Soon after, they achieved an isolated example of asymmetric reductive alkylation of aldehydes through synergistic photoredox and asymmetric chromium catalysis, producing chiral alcohols in 28% yield with 71% ee and complete linear selectivity.⁹⁵

6. Conclusion and outlook

Introducing organic photochemistry to asymmetric transition metal catalysis significantly revolutionized transition-metal-catalysed asymmetric coupling reactions. By doing so, chiral molecules can be facily assembled from inexpensive and abundant feedstock under extremely mild conditions. This review highlights the recent advances in this emerging and promising field by the joint use of visible-light photocatalysts and chiral transition metal catalysts. Notwithstanding these advances, several challenges have yet to be overcome. First, the key prochiral alkyl radicals captured by chiral metal catalysts are restricted to a few classes of stabilized radicals. It is highly desirable to expand to non-stabilized prochiral radical species. Second, to date, almost all reactions can be used for enantioselective C–C bond formation, and the realization of enantioselective C–N bond and C–O bond formation remains a significant challenge. Third, until now, BOX ligands have been widely utilized to synthesize chiral products and new powerful ligands should be explored quickly. Fourth, using or designing some suitable photocatalysts that can not only produce radical intermediates, but also adjust the valence of metal complexes is the key to the success of this type of reaction. Fifth, the generation rates of the radicals need to match the rates of radicals being captured by metal catalyst species, which is essential for the transformation in terms of reactivity and selectivity. Finally, novel reaction modes are expected from the

use of base metals such as manganese and iron in photoinduced asymmetric transformations.

Conflicts of interest

The authors declare no competing financial interest.

Acknowledgements

We are grateful to the National Science Foundation of China (No. 21822103, 21820102003, 21772052, 21772053 and 91956201), the Program of Introducing Talents of Discipline to Universities of China (111 Program, B17019), the Natural Science Foundation of Hubei Province (2017AHB047) and the International Joint Research Center for Intelligent Biosensing Technology and Health for supporting this research.

Notes and references

- J. Xuan and W.-J. Xiao, *Angew. Chem., Int. Ed.*, 2012, **51**, 6828–6838.
- C. K. Prier, D. A. Rankic and D. W. C. MacMillan, *Chem. Rev.*, 2013, **113**, 5322–5363.
- Y. Chen, L.-Q. Lu, D.-G. Yu, C.-J. Zhu and W.-J. Xiao, *Sci. China: Chem.*, 2019, **62**, 24–57.
- D. M. Schultz and T. P. Yoon, *Science*, 2014, **343**, 1239176.
- N. A. Romero and D. A. Nicewicz, *Chem. Rev.*, 2016, **116**, 10075–10166.
- D. Ravelli, S. Protti and M. Fagnoni, *Chem. Rev.*, 2016, **116**, 9850–9913.
- D. A. Nicewicz and D. W. C. MacMillan, *Science*, 2008, **322**, 77–80.
- D. A. DiRocco and T. Rovis, *J. Am. Chem. Soc.*, 2012, **134**, 8094–8097.
- R. S. J. Proctor, H. J. Davis and R. J. Phipps, *Science*, 2018, **360**, 419–422.
- Y. Yin, Y. Dai, H. Jia, J. Li, L. Bu, B. Qiao, X. Zhao and Z. Jiang, *J. Am. Chem. Soc.*, 2018, **140**, 6083–6087.
- H. H. Zhang, H. Chen, C. Zhu and S. Yu, *Sci. China: Chem.*, 2020, **63**, 637–647.
- A. Lipp, S. X. Badir and G. A. Molander, *Angew. Chem., Int. Ed.*, 2021, **60**, 1714–1726.
- L. Zhang and E. Meggers, *Acc. Chem. Res.*, 2017, **50**, 320–330.
- E. Arceo, I. D. Jurberg, A. Álvarez-Fernández and P. Melchiorre, *Nat. Chem.*, 2013, **5**, 750–756.
- R. Brimiouille, D. Lenhart, M. M. Maturi and T. Bach, *Angew. Chem., Int. Ed.*, 2015, **54**, 3872–3890.
- A. Ault, *J. Chem. Educ.*, 2002, **79**, 572–577.
- C. P. Casey, *J. Chem. Educ.*, 2006, **83**, 192–195.
- C. C. C. Johansson Seechurn, M. O. Kitching, T. J. Colacot and V. Snieckus, *Angew. Chem., Int. Ed.*, 2012, **51**, 5062–5085.
- M. R. Netherton and G. C. Fu, *Adv. Synth. Catal.*, 2004, **346**, 1525–1532.
- A. Rudolph and M. Lautens, *Angew. Chem., Int. Ed.*, 2009, **48**, 2656–2670.

- 21 J. F. Hartwig, *Organotransition Metal Chemistry: From Bonding to Catalysis*, University Science, Sausalito, CA, 2010, pp. 321–416.
- 22 G. C. Fu, *ACS Cent. Sci.*, 2017, **3**, 692–700.
- 23 J. B. Dicciani and T. Diao, *Trends Chem.*, 2019, **1**, 830–844.
- 24 S. Lou and G. C. Fu, *J. Am. Chem. Soc.*, 2010, **132**, 1264–1266.
- 25 H. Yin and G. C. Fu, *J. Am. Chem. Soc.*, 2019, **141**, 15433–15440.
- 26 Z. Wang, Z.-P. Yang and G. C. Fu, *Nat. Chem.*, 2021, **13**, 236–242.
- 27 J. C. Tellis, D. N. Primer and G. A. Molander, *Science*, 2014, **345**, 433–436.
- 28 Z. Zuo, D. T. Ahneman, L. Chu, J. A. Terrett, A. G. Doyle and D. W. C. MacMillan, *Science*, 2014, **435**, 437–440.
- 29 J. Amani, E. Sodagar and G. A. Molander, *Org. Lett.*, 2016, **18**, 732–735.
- 30 Z. Zuo, H. Cong, W. Li, J. Choi, G. C. Fu and D. W. C. MacMillan, *J. Am. Chem. Soc.*, 2016, **138**, 1832–1835.
- 31 C. Pezzetta, D. Bonifazi and R. W. M. Davidson, *Org. Lett.*, 2019, **21**, 8957–8961.
- 32 D. T. Ahneman and A. G. Doyle, *Chem. Sci.*, 2016, **7**, 7002–7006.
- 33 Y. Shen, Y. Gu and R. Martin, *J. Am. Chem. Soc.*, 2018, **140**, 12200–12209.
- 34 X. Cheng, H. Lu and Z. Lu, *Nat. Commun.*, 2019, **10**, 3549.
- 35 H. Guan, Q. Zhang, P. J. Walsh and J. Mao, *Angew. Chem., Int. Ed.*, 2020, **59**, 5172–5177.
- 36 P. Zheng, P. Zhou, D. Wang, W. Xu, H. Wang and T. Xu, *Nat. Commun.*, 2021, **12**, 1646.
- 37 Q.-Q. Zhou, F.-D. Lu, D. Liu, L.-Q. Lu and W.-J. Xiao, *Org. Chem. Front.*, 2018, **5**, 3098–3102.
- 38 E. E. Stache, T. Rovis and A. G. Doyle, *Angew. Chem., Int. Ed.*, 2017, **56**, 3679–3683.
- 39 P.-Z. Wang, J.-R. Chen and W.-J. Xiao, *Org. Biomol. Chem.*, 2019, **17**, 6936–6951.
- 40 E. Gandolfo, X. Tang, S. R. Roy and P. Melchiorre, *Angew. Chem., Int. Ed.*, 2019, **58**, 16854–16858.
- 41 P. Fan, Y. Lan, C. Zhang and C. Wang, *J. Am. Chem. Soc.*, 2020, **142**, 2180–2186.
- 42 X. Shu, L. Huan, Q. Huang and H. Huo, *J. Am. Chem. Soc.*, 2020, **142**, 19058–19064.
- 43 W. Ding, L.-Q. Lu, Q.-Q. Zhou, Y. Wei, J.-R. Chen and W.-J. Xiao, *J. Am. Chem. Soc.*, 2017, **139**, 63–66.
- 44 J. Liu, W. Ding, Q.-Q. Zhou, D. Liu, L.-Q. Lu and W.-J. Xiao, *Org. Lett.*, 2018, **20**, 461–464.
- 45 X. Shen, Y. Li, Z. Wen, S. Cao, X. Hou and L. Gong, *Chem. Sci.*, 2018, **9**, 4562–4568.
- 46 A. Gualandi, G. Rodeghiero, A. Faraone, F. Patuzzo, M. Marchini, F. Calogero, R. Perciaccante, T. P. Jansen, P. Ceroni and P. G. Cozzi, *Chem. Commun.*, 2019, **55**, 6838–6841.
- 47 L. Guo, F. Song, S. Zhu, H. Li and L. Chu, *Nat. Commun.*, 2018, **9**, 4543–4550.
- 48 L. Guo, H. Y. Tu, S. Zhu and L. Chu, *Org. Lett.*, 2019, **21**, 4771–4776.
- 49 H. Li, L. Guo, X. Feng, L. Huo, S. Zhu and L. Chu, *Chem. Sci.*, 2020, **11**, 4904–4910.
- 50 L. Huang, C. Zhu, L. Yi, H. Yue, R. Kancherla and M. Rueping, *Angew. Chem., Int. Ed.*, 2020, **59**, 457–464.
- 51 H. Yue, C. Zhu, R. Kancherla, F. Liu and M. Rueping, *Angew. Chem., Int. Ed.*, 2020, **59**, 5738–65746.
- 52 C. Zhu, H. Yue, B. Maity, I. Atodiresei, L. Cavallo and M. Rueping, *Nat. Catal.*, 2019, **2**, 678–687.
- 53 L. Guo, M. Yuan, Y. Zhang, F. Wang, S. Zhu, O. Gutierrez and L. Chu, *J. Am. Chem. Soc.*, 2020, **142**, 20390–20399.
- 54 S.-B. Lang, K. M. O'Nele and J. A. Tunge, *J. Am. Chem. Soc.*, 2014, **136**, 13606–13609.
- 55 J. Xuan, T.-T. Zeng, Z.-J. Feng, Q.-H. Deng, J.-R. Chen, L.-Q. Lu, W.-J. Xiao and H. Alper, *Angew. Chem., Int. Ed.*, 2015, **54**, 1625–1628.
- 56 S. B. Lang, K. M. O'Nele, J. T. Douglas and J. A. Tunge, *Chem. – Eur. J.*, 2015, **21**, 18589–18593.
- 57 H.-H. Zhang, J.-J. Zhao and S. Yu, *J. Am. Chem. Soc.*, 2018, **140**, 16914–16919.
- 58 H.-H. Zhang, J.-J. Zhao and S. Yu, *ACS Catal.*, 2020, **10**, 4710–4716.
- 59 X. Shen, L. Qian and S. Yu, *Sci. China: Chem.*, 2020, **63**, 687–691.
- 60 R. Trammell, K. Rajabimoghadam and I. Garcia-Bosch, *Chem. Rev.*, 2019, **119**, 2954–3031.
- 61 I. Perepichka, S. Kundu, Z. Hearne and C.-J. Li, *Org. Biomol. Chem.*, 2015, **13**, 447–451.
- 62 P. Querard, I. Perepichka, E. Zysman-Colman and C.-J. Li, *Beilstein J. Org. Chem.*, 2016, **12**, 2636–2643.
- 63 D. Wang, N. Zhu, P. Chen, Z. Lin and G. Liu, *J. Am. Chem. Soc.*, 2017, **139**, 15632–15635.
- 64 A. M. Hamlin, J. Cortez Fde, D. Lapointe and R. Sarpong, *Angew. Chem., Int. Ed.*, 2013, **52**, 4854–4857.
- 65 F.-D. Lu, D. Liu, L. Zhu, L.-Q. Lu, Q. Yang, Q.-Q. Zhou, Y. Wei, Y. Lan and W.-J. Xiao, *J. Am. Chem. Soc.*, 2019, **141**, 6167–6172.
- 66 H.-W. Chen, F.-D. Lu, Y. Cheng, Y. Jia, L.-Q. Lu and W.-J. Xiao, *Chin. J. Chem.*, 2020, **38**, 1671–1675.
- 67 Z.-L. Li, G.-C. Fang, Q.-S. Gu and X.-Y. Liu, *Chem. Soc. Rev.*, 2020, **49**, 32–48.
- 68 W. Sha, L. Deng, S. Ni, H. Mei, J. Han and Y. Pan, *ACS Catal.*, 2018, **8**, 7489–7494.
- 69 P.-Z. Wang, Y. Gao, J. Chen, X.-D. Huan, W.-J. Xiao and J.-R. Chen, *Nat. Commun.*, 2021, **12**, 1815.
- 70 F.-D. Lu, L.-Q. Lu, G.-F. He, J.-C. Bai and W.-J. Xiao, *J. Am. Chem. Soc.*, 2021, **143**, 4168–4173.
- 71 J. Chen, P.-Z. Wang, B. Lu, D. Liang, X.-Y. Yu, W.-J. Xiao and J.-R. Chen, *Org. Lett.*, 2019, **21**, 9763–9768.
- 72 T. Wang, Y.-N. Wang, R. Wang, B.-C. Zhang, C. Yang, Y.-L. Li and X.-S. Wang, *Nat. Commun.*, 2019, **10**, 5373.
- 73 J. Liu, X.-P. Liu, H. Wu, Y. Wei, F.-D. Lu, K.-R. Guo, Y. Cheng and W.-J. Xiao, *Chem. Commun.*, 2020, **56**, 11508–11511.
- 74 X. Bao, Q. Wang and J. Zhu, *Angew. Chem., Int. Ed.*, 2019, **58**, 2139–2143.
- 75 Z. Cheng, P. Chen and G. Liu, *Acta Chim. Sin.*, 2019, **77**, 856–860.
- 76 H. Chen, W. Jin and S. Yu, *Org. Lett.*, 2020, **22**, 5910–5914.
- 77 K. M. Nakafuku, Z. Zhang, E. A. Wappes, L. M. Stateman, A. D. Chen and D. A. Nagib, *Nat. Chem.*, 2020, **12**, 697–704.
- 78 Y. Li, M. Lei and L. Gong, *Nat. Catal.*, 2019, **2**, 1016–1026.

- 79 A. Hossain, A. Bhattacharyya and O. Reiser, *Science*, 2019, **364**, eaav9713.
- 80 Q. M. Kainz, C. D. Matier, A. Bartoszewicz, S. L. Zultanski, J. C. Peters and G. C. Fu, *Science*, 2016, **351**, 681–684.
- 81 C. Chen, J. C. Peters and G. C. Fu, *Nature*, 2021, **596**, 250–256.
- 82 X.-Y. Dong, Y.-F. Zhang, C.-L. Ma, Q.-S. Gu, F.-L. Wang, Z.-L. Li, S.-P. Jiang and X.-Y. Liu, *Nat. Chem.*, 2019, **11**, 1158–1166.
- 83 X.-Y. Dong, J.-T. Cheng, Y.-F. Zhang, Z.-L. Li, T.-Y. Zhan, J.-J. Chen, F.-L. Wang, N.-Y. Yang, L. Ye, Q.-S. Gu and X.-Y. Liu, *J. Am. Chem. Soc.*, 2020, **142**, 9501–9509.
- 84 H.-D. Xia, Z.-L. Li, Q.-S. Gu, X.-Y. Dong, J.-H. Fang, X.-Y. Du, L.-L. Wang and X.-Y. Liu, *Angew. Chem., Int. Ed.*, 2020, **59**, 16926–16932.
- 85 Y. Zhang, Y. Sun, B. Chen, M. Xu, C. Li, D. Zhang and G. Zhang, *Org. Lett.*, 2020, **22**, 1490–1494.
- 86 C. Li, B. Chen, X. Ma, X. Mo and G. Zhang, *Angew. Chem., Int. Ed.*, 2021, **60**, 2130–2134.
- 87 Q. Guo, M. Wang, Q. Peng, Y. Huo, Q. Liu, R. Wang and Z. Xu, *ACS Catal.*, 2019, **9**, 4470–4476.
- 88 Y. Li, K. Zhou, Z. Wen, S. Cao, X. Shen, M. Lei and L. Gong, *J. Am. Chem. Soc.*, 2018, **140**, 15850–15858.
- 89 B. Han, Y. Li, Y. Yu and L. Gong, *Nat. Commun.*, 2019, **10**, 3804.
- 90 K. Zhou, Y. Yu, Y.-M. Lin, Y. Li and L. Gong, *Green Chem.*, 2020, **22**, 4597–4603.
- 91 J. L. Schwarz, F. Schäfers, A. Tlahuext-Aca, L. Lückemeier and F. Glorius, *J. Am. Chem. Soc.*, 2018, **140**, 12705–12709.
- 92 H. Mitsunuma, S. Tanabe, H. Fuse, K. Ohkubo and M. Kanai, *Chem. Sci.*, 2019, **10**, 3459–3465.
- 93 J. L. Schwarz, H. M. Huang, T. O. Paulisch and F. Glorius, *ACS Catal.*, 2020, **10**, 1621–1627.
- 94 S. Tanabe, H. Mitsunuma and M. Kanai, *J. Am. Chem. Soc.*, 2020, **142**, 12374–12381.
- 95 Y. Hirao, Y. Katayama, H. Mitsunuma and M. Kanai, *Org. Lett.*, 2020, **22**, 8584–8588.